# POLITECNICO DI TORINO

MASTER's Degree in MECHATRONICS ENGINEERING

MASTER's Degree Thesis

# MULTICHANNEL AUTO-RANGED CURRENT SENSING FOR AUTOMOTIVE CONTROL UNITS

**Supervisor**

Prof. Paolo Stefano CROVETTI

Company Tutor: Valerio SABATINI

**Candidate**

Matteo VOTTERO VIUTRELLA

**2021/2022**

*Alla mia famiglia*

# Abstract

Thanks to the development of the vehicle technologies and the introduction of new features, automotive ECUs can absorb a very wide range of current during their normal activity, depending on the different operational conditions (workload or active functionalities). In the ECUs testing activities it is fundamental to monitor the power consumption, to verify if the current draining is compatible with the vehicle operating conditions.

Most commercial solutions do not allow to measure the current drain in the whole operating range with the required accuracy, and their integration in automated testing solutions is often not possible. From this need, there is a growing interest in developing a custom solution to measure a wide current range with a high accuracy.

The final target of this thesis is to design and build a device that can meet the aforementioned requirements on four channels. For this purpose, different sensor technologies have been compared and analyzed. The two main technologies, which have been employed in the final system, are based on the volt-amperometric method (shunt resistor), and on the magnetic induction field sensing (Hall-Effect sensor). Advantages, disadvantages and finally yet importantly the limit of each instrument have been compared, to understand what is the best solution to cover the desired range.

Lastly, the device must be able to switch automatically between different ranges, to guarantee the proper accuracy. Moreover, the sensed measurements need to be transmitted to the automatic testing equipment via serial interface and on CAN bus for further processing.

# Table of Contents

# List of Tables

# List of Figures

# Acronyms

**DC** Direct Current

**AC** Alternating Current

**CAN** Controller Area Network

**ADC** Analog to Digital Converter

**PWM** Pulse With Modulation

**DAC** Digital to Analog Converter

**PCB** Printed Circuit Board

**TI** Texas Instrument

**GND** Ground

**ECU** Electronic Control Unit

**CAD** Computer Aided Drafting

**ECAD** Electronic Design Automation

**HIL** Hardware In the Loop

**SSR** Solid State Relay

**MOS** Metal-Oxide-Semiconductor Field-Effect Transistor

**LV** High Voltage

**LV** Low Voltage

**OLED** Organic Light-Emitting Diode

**I2C** Inter Integrated Circuit

**SDA** Serial Data line

**SCL** Serial Clock Line

**SPI** Serial Peripheral Interface

**ID** Identifier

**DLC** Data Lenght Code

**SI** System of Units

**SAR** Successive Approximation

**SMD** Surface Mounted Devices

# Chapter 1

# Introduction

## 1.1 Current sensing project

This thesis was developed in co-operation with the Italdesign Giugiaro S.p.a. company, which wants to find a solution that can be implemented in the automotive testing environment. This new device should be able to monitor automatically the current flowing inside the ECUs and it will be implemented in the testing environment. Full-filling not only the requirements and the need of the Italdesign company, but by tuning and changing the proper components can be employed in different automotive applications. Since the automotive control units have several working conditions, this device should be able to sense automatically a huge range of currents, especially paying attention to the low range. In the case of Italdesign, the infotainment control unit can span from the sleep state, which drains a few tens of microampere, up to the ON state where the current can be higher than five amperes. During testing activities, the sensed current is required for monitoring the power consumption of the hardware and the different functionalities. In this context it has been decided to proceed with this thesis activity. A key feature that should be implemented on the final device is the possibility to communicate in real time with the user and testing equipment. In addition, in order to monitor different control units, multiple sensed channels are required. (Fig 1.1).

The project is divided in different steps: requirements analysis according to the performed experimental tests, examination of the different current transducer technologies, design trials, prototype design and lastly the concept and testing of the final device.

**Requirements analysis:** In this first phase of the project, different experimental tests have been done for each operating condition such sleep, stand-by and ON

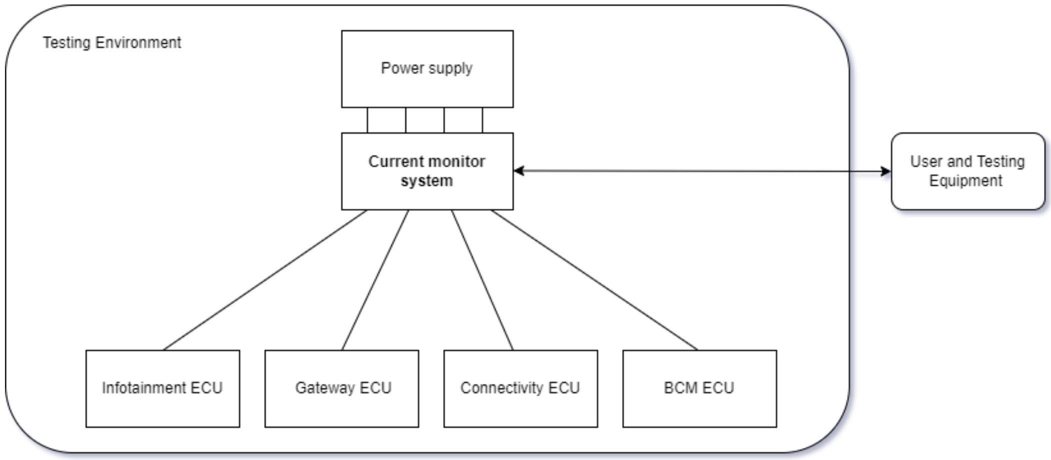


**Figure 1.1:** Example scheme

states. This was done to obtain an overview of the requirements to fulfill and to realize the full range of measure. An oscilloscope with a shunt transducer has been used to perform the measurements and the acquired data has been processed by a custom program developed in Phyton.

**Review of the different current transducer technologies:** In the second phase of the project, a research of the current sensing techniques has been done, examining all the available technologies. Due to the automotive control units peculiarity, the measurement of direct current has been deepened. In this context, the analysis revealed that the most suitable techniques are the Volt-Amperometric method and the Hall-effect based current sensing.
Thereafter, the main current sensing solutions on the market have been examined. This is done to take inspiration and to optimize the working principles of the existing devices. Different factors have been taken into account during the design phase such as budget, circuitry simplicity, communication and the control effectiveness. The final target is to find a perfect trade-off between these factors, using a simple circuit with fast and reliable system control. The final solution should be fully customizable, depending on each company needs.

**Design trials:** In the third stage, different concept boards have been designed, especially taking into account of the limits and drawbacks of each configuration. Three different structures were developed (figure 1.2).

The first structure was composed by the series of two shunt resistors. In this configuration, a power switch is required to short-circuit one resistor during high

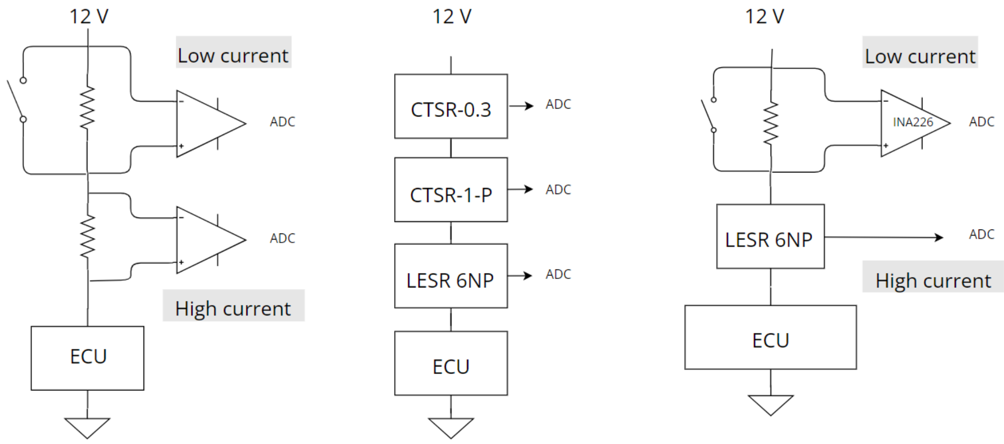


**Figure 1.2:** Simplified scheme of the three concept boards

current drain conditions. In this case it was not possible to meet at the same time the requested accuracy and the burden voltage limitations. By using only two resistors, also tuning the gain of the current sensing monitor device, it was not able to provide a voltage-output that was within the limits of the Arduino ADC. In addition, increasing the value of the resistors, the burden voltage overcomes the imposed limits in the upper current range.
The second one was based on three hall effect transducers in series. Apparently, it was the most straightforward solution, since it did not need any switch to protect the acquisition system, thus simplifying the control and the data processing. However, it did not satisfy the requirement of accuracy in the low current range.
The last case was a sensor fusion configuration composed by a shunt resistor, assigned to the low current range, and two Hall transducers used to sense high currents. This structure almost met the requirements, consequently it has been improved and later used for the final design. The circuit design was followed by an optimization phase, leading to the final solution. Finally the prototype has been developed.

**Prototype:** In this stage the prototype was built. In particular it was a mono-channel sensor fusion device, constituted by two different transducers: a Hall sensor and a Shunt resistor with the corresponding current monitor device. The whole algorithm was developed in the Arduino IDE including the data processing, switching control logic, CAN communication and OLED display control. The schematic and the printed board scheme have been developed. Subsequently the fabrication of the prototype .

**Final design:** The final system was designed improving the prototype structure and algorithm. This configuration is engineered to sense the current on four different channels. Subsequently, the data are sent on CAN and at the same time showed up on an OLED display. The prototype algorithm was revised and speed up in order to be compatible with the micro-controller computational power. The electrical scheme and final printed board scheme were developed. Due to the global components shortage, the final printed board was not available for the final experimental tests.

In conclusion, starting from the requirements a multi-channel device has been developed, it is able to sense the current coming from different control units that deal with different functionalities such as display operation, connectivity, and other infotainment services. Subsequently after the proper data processing the final results will be sent on CAN and displayed for testing purpose.

## 1.2 Italdesign Giugiaro S.p.A

**Figure 1.3:** Company logo

Italdesign is a service company providing design, engineering and production for the transportation industry, through to final testing and type-approval and support into starting of production and the design of complete Business models. [1]

In particular the project has been developed in the Testing & Validation department. This team acts as a service layer for all the departments and projects requiring modelling, testing and validation activities. Different test cases are developed starting from the customer needs. This team is able to take the responsibility for the complete infotainment and connectivity systems development and integration into customer platforms.

# Chapter 2

# State of Art

Definition of Electric current: “An electric current is a stream of charged particles, such as electrons or ions, moving through an electrical conductor or space. It is measured as the net rate of flow of electric charge through a surface.” [2]

## 2.1 Current sensing: history and initial applications

Since the beginning of the electrical engineering, there was the willing (and the need) to measure the amount of current that flows into a wire. Besides the electrical current also other electrical units are considered, such the electromagnetic field quantities and the voltage.
At the origin, the joule’s heat, the force generated by a magnetic field or other physical effects associated with the flow of electrons inside a wire, provoked the interest of the engineers for understanding the physical working principle. As a consequence the first current sensing instrument was the combination of a transducer and the display on a inseparable measurement unit.
Towards the end of the $19^{th}$ century, the advancement of technology and the increment of the current intensity, made it difficult to measure the current directly. From this came the need to build a different solution that led to the “first current transducer”.
In 1837 the tangent galvanometer Fig 2.1 has been designed, it was a simple compass affected by the magnetic field of a current passing into a wire, the needle was left free to move in the earth’s magnetic field. In 1884 the first shunt measurement was made from a copper conductor, this allowed to increase the range up to 200 A, a few years later in the 1893, higher current measurements have already been done, reaching intensity above 10 kA. Since these circuits did not have specific

**Figure 2.1:** Tangent galvanometer

protections, or conditioning circuits, the results of these first instruments were often compromised by the temperature and by the external magnetic field. In 1901, the first transformer with a partially decoupling between primary and secondary circuit, was built. In the following years the current sensing instruments were refined, gaining improvements on the measuring range and on the accuracy, the first device able to sense large DC current with a elevated accuracy was built in the 1939 by Krämer (Fig 2.2), it could reach up to 30 kA with 0,5% of accuracy. Beginning in 1879, the advancement of instruments based on the measure of small magnetic field had begun, the so called Hall-effect sensor. Only in 1950 the technologies allowed the construction. Parallel with the development of the inductive current transducers, also the instrument based on the shunt resistances were carried out. In the following years, other technologies based on the the indirect current measure have been inspected such as: Faraday effect, magneto-impedance, magneto-resistance or nuclear magnetic resonance (NMR) [3].

## 2.2 Overview on the different methods

The current sensing challenge is a widely common and quite important task in electronics and the electricity fields. For the complete design of the device it is necessary to take into account different information: such as the current type, the

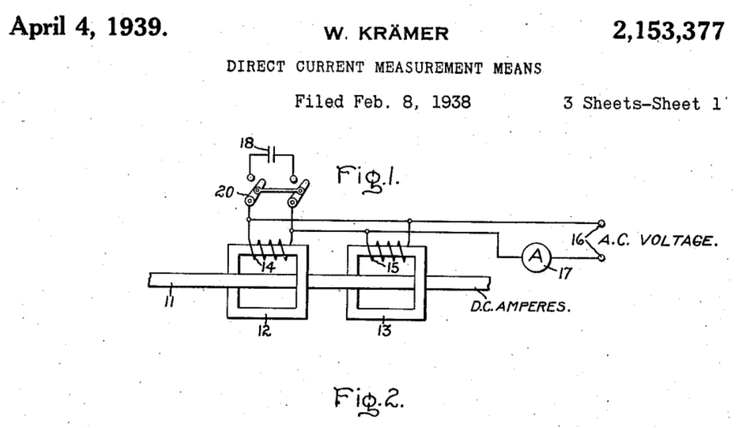


**Figure 2.2:** Kramer solution

applications, the permitted burden voltage induced by the measuring instrument, the desired range, the sensitivity, the accuracy and many other factors. The measuring process is composed by different stages: as first the current is sensed, depending on the current intensity there could be necessary an amplification step and secondly the conditioning circuit to obtain the final result depending on the desire output (directly displayed or digitally transmitted for control system purpose).

The target of this chapter is to analyze and study more in depth the actual current sensor techniques, to understand what is the best solution for the application of this project. Aiming to pay special attention on the the working principle and on the main advantages/disadvantages of the different technologies. The following method have been considered:

1. Ohm's law applied on a resistance
2. Sensors based on the electromagnetic field

### 2.2.1 Ohm's law applied on a resistance

The ohm's law applied on a resistor is a reduction of the Lorentz law:

$$\boldsymbol{J} = \sigma(\boldsymbol{E} + \boldsymbol{v} \wedge \boldsymbol{B}) \tag{2.1}$$

**J** current density, **E** electric field, **v** the velocity of the charges, **B** the magnetic flux density that acts on the charge and as last $\sigma$ is the conductivity of the material. The second term is negligible, unless a strong magnetic induction field is applied, this leads to the simplification:

$$\boldsymbol{J} = \sigma \boldsymbol{E} \tag{2.2}$$

The equation above is the so-called Ohm's law, it is possible to notice that the drop voltage across the resistor is current proportional, the current sensing on the resistor is based on this very simple statement.

**Shunt resistor:** The name comes from the verb "to shunt" that means to follow a different path or to turn away. It is a very common and classic approach due to the easy implementation. As mentioned above, the voltage drop across the resistor is proportional to the current that flows inside it. An advantage of this device is the possibility to sense both types of current, alternating (AC) and direct (DC), and one of the main disadvantages is the large voltage drop generated with high current, consequently high power losses and Joule's effect are induced.

*Joule's heating* is associated to the temperature increasing, induced by the current flow inside a device. Electrical energy is transformed into thermal energy through the law of the conservation of energy (eq 2.3):

$$H(t) = I^2 R \tag{2.3}$$

$H$ is the heat produced by the conductor during a certain time period $t$, $I$ and $R$ are respectively the electrical current and the resistance. The amount of heat $Q$ produced after a time $t$ is given by 2.4:

$$Q = Pt \tag{2.4}$$

$P$ is the dissipated power. The temperature increasing $T$ is given by 2.5:

$$T = Qcm \tag{2.5}$$

where $m$ is the conductor mass and $c$ is the specific heat of the material [4].

Another significant drawback of the shunt resistor technique is that most of the time, it is mandatory to use an amplifier to gain the signal to be sent to the acquisition system. This is due to the very low voltage value across the shunt resistor, as a result of low currents. In these cases the amplifier is calibrated to satisfy the input swing of the acquisition system. (Example: if the maximum burden voltage across the resistor is 0.1 V and the ADC is 0-5 V, the gain of the amplifier will be 50 to be within the range). It also important to take in consideration the minimum sensitivity of the instrument, which is dependent on the number of bit and on the voltage reference of the acquisition system.

$$ADCresolution = \frac{V_r}{2^n} \tag{2.6}$$

Where $V_r$ is the internal reference voltage used by the ADC for the conversion, $n$ is the number of bit.
The problems described above are among the most significant limits of the shunt resistor technology, which restrict the range of utilization.

Following will be described the two most widespread methods that employ the shunt resistor technique.

- Coaxial Shunt resistor:
  Some applications require to measure transient current pulses with high amplitude and a huge rise times, as a consequence the frequency behavior of the resistor is crucial for this application. The shunt resistor could be represented with an equivalent circuit (fig 2.3).

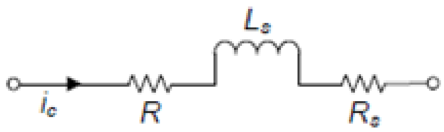


**Figure 2.3:** Equivalent circuit for a shunt resistor

  Where $R$ is the nominal value of the resistor, $L_s$ represents the parasitic inductance and $R_s$ is given by the skin effect. $L_s$ is the responsible of the bandwidth decrement, it is given by the mutual inductance $M$ between the loop induced by sensing wires and the loop induced by the main current. The connection is very important to reduce this effect and increase the performance. The solution is a coaxial resistive tube that decreases the parasitic inductance reducing the flux generated into the sensing wires.
  $R_s$ as mentioned above, is induced by the *skin effect*, which is a phenomena dependent on the size of the conductor and on the intensity of the alternating current. Whereby, the current density is not equally distributed along the conductor, it is greater towards the external surface and decreases exponentially towards the center of the conductor. As a consequence, this problem decreases the available section inside the conductive element, increasing the effective value of resistance.

$$J = J_s e^{-(1+j)\frac{d}{\delta}} \tag{2.7}$$

  $J$ is the alternating current density in a conductor, $J_s$ is the value of the current density at the surface, $d$ is the depth from the surface and $\delta$ is the skin depth.

$$\delta = \sqrt{\frac{2\rho}{\omega\mu}}\sqrt{\sqrt{1+(\rho\omega\epsilon)^2}+\rho\omega\epsilon} \tag{2.8}$$

where $\rho$ is the resistivity, $\omega$ is the angular frequency, $\mu$ is the permeability (composed by the multiplication of $\mu_r$ the magnetic permeability and $\mu_0$ the free space permeability), $\epsilon$ is the permittivity of the conductor (composed by the multiplication of $\epsilon_r$ the relative permittivity and $\epsilon_0$ the free space permittivity).

Due to the coaxial construction (to ensure low parasitic inductance) the skin effect is not negligible, when the magnitude of the current pulses are in the range of 100 kA the skin effect is the responsible of the bandwidth decrement [5]. In certain cases, it has been found that the induced voltage (burden voltage) compensates the skin effect. [6]

- Surface Mounted shunt resistor:
  Coaxial shunt is not the right choice in the integrated devices environment, due to their size and cost, their use is related to current with high frequency and significant magnitude.
  In these cases the shunt resistor must have small size and it should be able to be mount onto surface-mounted-devices (SMD). The current range for this kind of devices reaches a magnitude up to 100-200 A. Exceeding this limit the losses become significant, consequently, it comes the need to dissipate high power, increasing the size of the devices.
  In the case of SMD integrated shunt resistor, due to the small physical size required for the integration, the skin effect becomes negligible. Therefore the equivalent circuit could be represented by only the series of $R$ and $L_s$. [6]
  It can be seen from the figure 2.4 that the frequency response has a significant

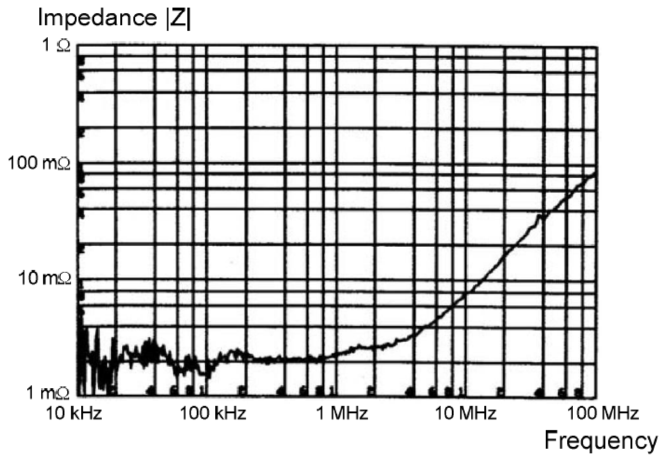


**Figure 2.4:** SMD Impedance measurement (WSL2512, 3 mohm - Vishay)

impact on the impedance of the Shunt resistor. During the design, this range has to be taken in consideration, it is given by the manufacturer. Overcoming the corner frequency, the impedance value increases rapidly with a slope of 20 dB/dec, this value can be predicted using the following formula (the skin effect is considered negligible).

$$f_c = \frac{R}{2\pi L_s} \tag{2.9}$$

The last important peculiarity that should be noted is the thermal drift. Typically shunt resistors are made of a material with low temperature coefficient of resistivity, as nickel-crome and manganese copper alloys, they can reach low values of temperature coefficient of resistance (<20 ppm/K). The welding temperature coefficient between the surface of the printed board and the shunt resistor is the main problem. With very low values of shunt resistance this problem is accentuated, the thermal drift is compromised by the temperature coefficient of the welding. To solve the problem sophisticated shunt resistors are employed by using the four-wire Kelvin principle.

The *four-wire Kelvin principle* is a dedicated sensing technique, used to find very low resistance value ($< 0{,}1\ \Omega$) or for current measurements with high accuracy. It is used especially to prevent errors caused by the resistance value of the wires. Two wires are used for the current supply, and the second pair of wires is used for the sensing of the voltage drop across the measuring resistor (figure 2.5). Hence, the key feature is the fact that any voltage drop induced by the leads, has not effect on the voltage drop sensed across the resistor. This is related to the fact, that the two sense pins are placed adjacent the measuring resistor, in this way the wire resistance does not affect the final impedance result.

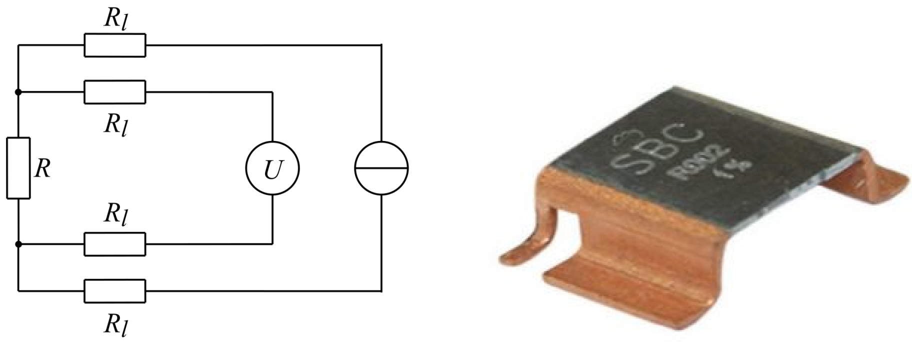


**Figure 2.5:** 4 wire principle

Low side and High side monitoring

Before selecting the correct value of the shunt, it is required to decide where to place the resistor: between the supply voltage and the load (High side monitoring) or between the load and the ground (Low side monitoring). There are some differences between the two methods, some advantages and disadvantages.

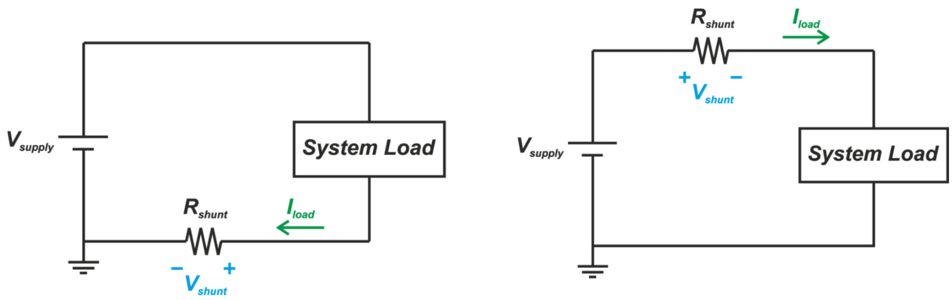


**Figure 2.6:** Low-side monitoring (Left) and High-side monitoring (Right) [7]

- *Low side* sensing: as mentioned before in this configuration the shunt resistor is located between the load and the ground. In most of the case, this configuration is the simplest and less expensive one, due to the fact that one pin of the resistor is connected to the ground side of the load and the other pin is connected at system ground. Hence, since the voltage drop is low, it can be directly acquired by using simple analog to digital converter.
  The most common issue with this configuration is the potential ground loop problem. Since the load is not at the same ground potential of the other loads in the system, the system can develop interference with nearby equipment. This configuration fits better in the systems composed by one single load [8]. Furthermore this configuration is not able to detect fault conditions such short or open circuit (figure 2.7). As it can be seen from the figure in case of short circuit, the current flows directly through the system ground, without passing through the low side shunt. This happens in both cases: short circuit between the supply and the load and short circuit between the load and the system ground.

- *High side* sensing: as mentioned before in this configuration the sense resistor is placed between the supply and the load. This method has a better responsiveness to the current flow changes and it does not add fluctuations or disturbances such the low side case ([6]). The main disadvantage is related to the fact that the shunt resistor is connected directly with the supply voltage, this means that dedicated devices are required (such the high side current shunt monitor). This kind of device can work with very high common mode

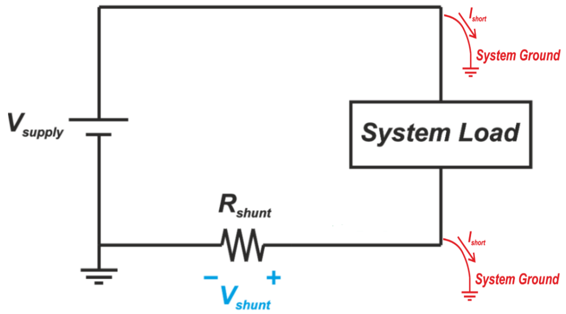


**Figure 2.7:** Low side ground loop [7]

voltage (i.e. up to 80 V). The advantage of this configuration is the ability to detect faults in the system (short or open circuit), as it can be seen from the figure (2.8). In the case of failure, the short circuit current flows through the high side shunt, in both failure cases (before and after the load).

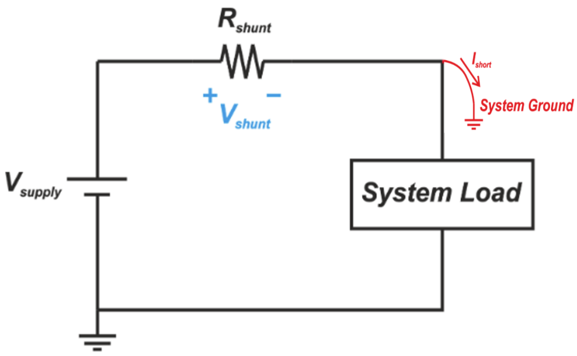


**Figure 2.8:** High side shunt detection[7]

Following, will be described techniques that apply Ohm's law without using a dedicated shunt resistor, but exploiting the intrinsic resistance of a conductor element in the circuit.

- Internal Resistance of a MOSFET:
  Besides the previous technique in power electronics , the MOSFET $\mathbf{R}_{ds,on}$ is used as a linear resistance to employ in the current sensing technique (fig 2.9).

$$R_{DS} = \frac{l}{W\mu C_{OX}(V_{GS} - V_T)} \tag{2.10}$$

  where $l$ is the length of the channel, $W$ is the width of the channel, $\mu$ is the mobility of the carrier, $C_{OX}$ is the capacitance of the gate oxide and $V_T$ is is the threshold voltage. The current is obtained, by measuring the voltage between the drain and the source. When the MOS is conducing, it is possible to measure the current, by applying the Ohm's law:

$$i_S = \frac{V_{SENSE}}{R_{DS}} \tag{2.11}$$

The main problems connected to this kind of component are: firstly the device-to-device variation of the $R_{ds,on}$ leading to a frequent re-calibration and secondly the considerable thermal drift. This leads to a higher circuit complexity and higher costs, linked with the need to use specific components to sense the induced voltage. For these reasons, this technique can not fit solutions that require high accuracy.

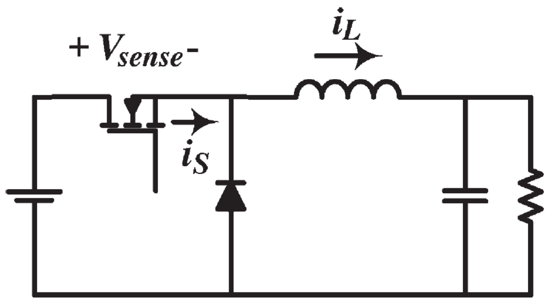


**Figure 2.9:** $R_{DS}$ circuit based[9]

- Copper trace resistance sensing in PCB:
  It is feasible to use the natural resistance value of the copper trace in the PCB instead of using a specific shunt resistor. This approach does not introduce any power losses, but the resistance value of the trace is very low (eq 2.12).

  $$R(T) = \frac{S(T) \cdot l}{a} \tag{2.12}$$

  $R$ is the resistance; $S(T)$ is the resistivity $[\Omega \cdot cm]$ equal to 1,7214 $\times 10^{-6}$, for a typical copper; $l$ is the length [cm]; $a$ is the Area $[cm^2]$. The resistivity is a function of the temperature. The corresponding sensed voltage is infinitesimal. For this reason current monitor device with high gain are required.
  In the article of Spaziani [10], it is shown the large dependence on the thermal drift. This technique is used in power converter applications, and it needs at least 20% of the rated nominal current to work properly. This method is not recommended for high accuracy application.

- <u>Inductor internal resistance:</u>
  In power electronics, to avoid the use of an additional resistor, it is also possible to employ the inductors for current sensing. The inductor has an internal resistance $R_L$ and is magnetically coupled with an identical inductor (with equal number of turns)(fig 2.10).
  The voltage drop across the main inductor is composed by $V_1$ and $V_2$:

$$V_L = V_1 + V_2 = L\frac{di_L}{dt} + i_L R_L \tag{2.13}$$

  With a minimum current flow, the extra winding is coupled with the main inductor. Due to the equal number of turns, the voltage on both windings is equal. As a consequence, if the two voltages are subtracted, the resulting voltage is proportional to the current flow $i_L R_L$.
  Due to the strong noise and thermal drift susceptibility, this technique is used mostly for low-voltage high-current power converter applications [9].

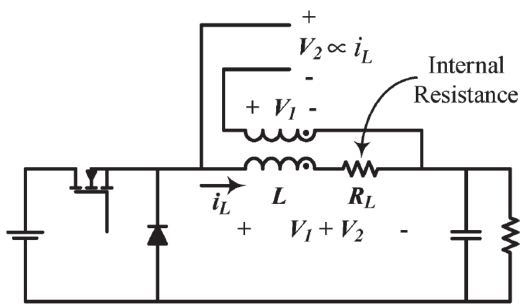


**Figure 2.10:** Current sensing on the inductor [9]

### 2.2.2 Sensors based on the electromagnetic field

This kind of sensors is able to measure the intensity of static and dynamic magnetic fields, induced by the current flowing into the wires. Usually, this type of devices are employed in high-power applications, where the isolation is suitable. There exist different techniques based on this principle, in this chapter are deepened the most widespread. These technologies can be distinguished for the different accuracy level, type of sensed current (DC or AC) and the architecture.

**Rogowski coil:** In this technique, the conductor passes through an air (or ironless) solenoids with hundreds or thousands of turns, the voltage-output of the Rogowski coil is then connected with an electrical integrator (fig 2.11).

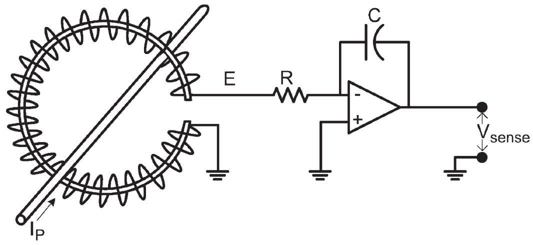


**Figure 2.11:** Rogowski coil simplified scheme [9]

The magnetic field induced by the current flow, generates a voltage drop $E$ in the secondary coil, which varies proportionally with the rate of change of the primary current:

$$E = M\frac{dI_p}{dt} \tag{2.14}$$

$M$ is the mutual inductance of the circuit, $I_p$ is the intensity of the primary current. $M$ is dependent on the intrinsic parameters of the coil:

$$M = \frac{\mu_0 A N_S}{l} \tag{2.15}$$

where $\mu_0$ is the free space permeability, $A$ is the cross section of the coil, $N_S$ is the number of turns in the secondary winding and $l$ is the mean path length of the coil. Lastly, the output voltage of the integrator is proportional to the primary current:

$$V_{SENSE} = \frac{1}{RC}\int E \cdot dt = \frac{1}{RC}\frac{\mu_0 A N_S}{l} I_P \tag{2.16}$$

Since the air core will not saturate, the output of this kind of device remains linear also for high-current measurement. In addition, the derivative of the DC current is zero, hence this type of device can measure only AC or pulsed DC.

One of the main advantage, it is the possibility to place the conductor inside the coil without interrupting the main circuit.
The opening in the structure leads to errors (between the 1% and 2%), these are dependent on the conductor position inside the hole. Furthermore, the accuracy is influenced by the external magnetic field.

**Hall Effect Sensor:** This is the most spread magnetic field reading technology for current sensing, it is based on the Hall effect (found out by Edwin Hall 1879). Current measurements built on this principle are mainly employed for DC or AC, thanks to their configuration.
When a current $I$ flows through a thin sheet of conductive material penetrated by a magnetic flux density $B$, a voltage $v$ is generated perpendicular to both, the current and field.

$$v = \frac{IB}{nqd} \tag{2.17}$$

Where $q$ is the charge of current carrier, $n$ is the carrier density and the $d$ the thickness of the sheet. [6]
It is worth to say that the Hall Effect is explained by the second term of the Lorentz equation, the one that was negligible in the previous section. The induced voltage by the hall element is bidirectional, it can be produced on both senses, positive and negative one. The hall coefficient is indicated as $R_H$:

$$R_H = \frac{1}{nq} \tag{2.18}$$

The most used materials for the construction of the Hall components are gallium arsenide (GaAs) and Indium antimonide (InSb).
The ohmic resistance is an important parameter, it defines the power loss occurring inside the sensor. Consequently, there is a balancing between the Hall plate thickness, which is responsible of the sensitivity, and the Hall plate resistance.
Hall effect sensor are subject to an offset voltage, that could be eliminated by using additional circuitry.
The main disadvantages of this transducer type are: limited linearity range, sensitivity to mechanical stresses (and temperature variation) and also the limited maximum frequency. These drawbacks can be overcame using appropriate configurations, such open loop and closed loop.

Open loop configuration: The main advantages of this configuration are the simplicity, the compactness and the cost. Mainly the intensity of the magnetic field is supposed linear with the current change. Anyway the linearity, sensitivity and the thermal drift are calculated by using the principle of magnetic field sensing. To reach high accuracy, is necessary a proper calibration which needs to find the proportionality factor between the current magnitude and the intensity of the magnetic field. Due to the small output voltage coming from the Hall sensor, it is required an amplification stage (fig 2.12). For this reason the bandwidth of the instrument is dependent not only on the hall element but also on the bandwidth of the amplification stage. Clearly the biggest problem in this type of device are the external magnetic fields, it is possible to shield the sensor from the external signals but this procedure influences the final measurement, also by limiting the final bandwidth. The device performance are dependent also on the magnetic core proprieties, overcoming the appropriate bandwidth leads to overheating. As last, it is worth to say that an excessive over-current situation could affect the magnetic core proprieties, changing the working point and the device characteristics.

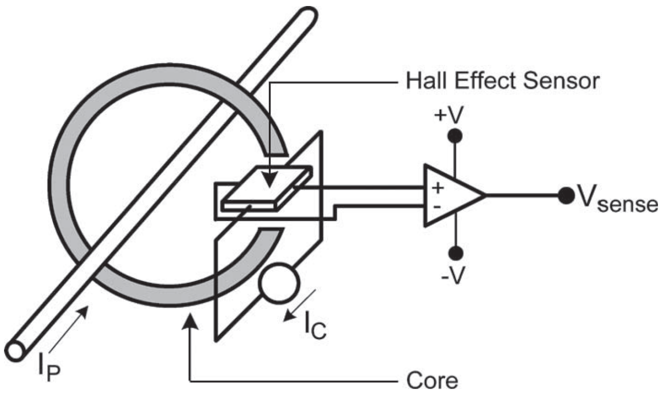


**Figure 2.12:** Open loop configuration [9]

Closed loop configuration: By using a compensation circuit, the performance of the open-loop configuration are increased (fig 2.13). This structure is based on the concept of the negative feedback, the output voltage of the magnetic field sensor is used as an error signal to compensate the magnetization inside the magnetic core by forcing a current $i_s$ through a second transformer winding [6]. This current needs to induce an opposite magnetic field to compensate the one developed by $i_p$.
The Hall sensor generates a voltage proportional to the flux density in the core.
The benefit is the reduction of the thermal-drift influence, that leads to the independence between the linearity and the magnetic field sensor. The second big advantage is a huge increment in the bandwidth, thanks to the fact that in the high frequency range, the secondary winding works as a current transducer, obtaining a wider frequency range.
Clearly this technology leads to higher costs, due to the higher complexity, and limited output current due to the fact that closed-loop sensors can only drive a finite amount of secondary current.

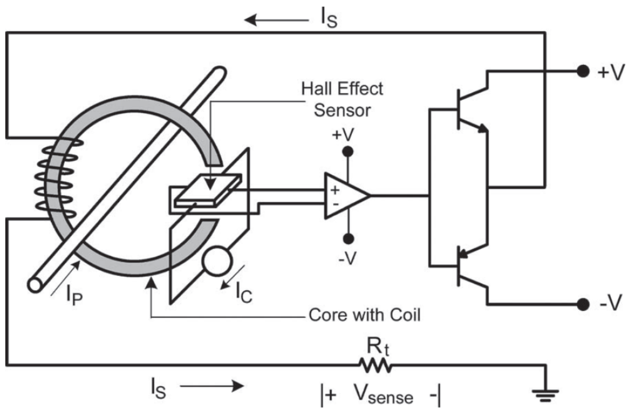


**Figure 2.13:** Closed loop configuration [9]

In conclusion, this type of sensor is extensively spread thanks to the electrical isolation between the sensed current and the final output voltage. However, an appropriate accuracy is dependent on high costs and circuitry complexity. Lastly the two main limitations using this technology are the over-current degradation and the thermal output dependence.

**Fluxgate Principle:** The Fluxgate principle is based on the non-linear relation between the magnetic field $H$ and the magnetic flux density $B$, within a magnetic material. In the figure 2.14, it is shown the the Vacquier fluxgate sensor.

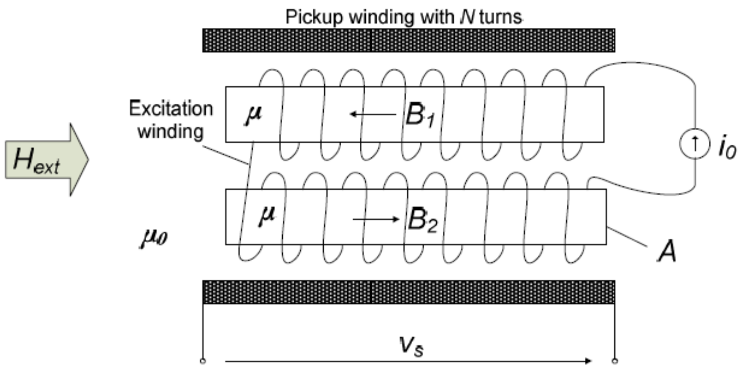


**Figure 2.14:** Fluxgate principle [6]

The excitation winding gives rise to an excitation field $H_0$ that drives the magnetization of the two parallel rods periodically between positive and negative values [6]. Since the excitation fields in the two rods are directed in opposite directions, the

the pick-up winding wound around the two rods does not see the magnetic field generated by the excitation winding. The generated voltage $V_S$ into the pick-up winding is equal to:

$$V_S = -2NA(\frac{dB_1}{dt} + \frac{dB_2}{dt}) \tag{2.19}$$

$N$ is the turns number on the pick-up winding; $A$ is the section. To drive the excitation winding is used a sinusoidal current $i_0$, the permeability $\mu$ corresponds to the $B$ rate of change, in each of the cores.

$$\mu = \frac{dB_{Hext \pm H_0}}{d(H_{ext} \pm H_0)} \tag{2.20}$$

Combining the two previous equations:

$$V_S = -2NA(\mu_1 \frac{d(H_{ext} + H_0)}{dt} + \mu_2 \frac{d(H_{ext} - H_0)}{dt}) \tag{2.21}$$

In the case of static magnetic field:

$$V_S = -2NA\frac{dH_0}{dt}(\mu_1 - \mu_2) \tag{2.22}$$

Differential permeability $\mu_d$:

$$\mu_d = \mu_1 - \mu_2 = (\frac{dB_{H+H_0}}{d(H_{ext} + H_0)} + \frac{dB_{H-H_0}}{d(H_{ext} + H_0)}) \tag{2.23}$$

The differential permeability is time dependent due to the changes in the excitation field $H_0$. Finally:

$$V_S = -2NA\mu_d \frac{dH_0}{dt} \tag{2.24}$$

To increase the sensitivity is possible to increase the number of turns in the pick-up winding, use higher excitation current frequency or a core with a fast change permeability.
Other fluxgate principles besides the Vacquier one are known.
The fluxgate sensor has a very reliable sensitivity, they can be used in closed-loop and open-loop configuration. The main difference between the Hall effect sensor and the Flux gate sensor is the core material, respectively the first uses air core and the second uses a saturable inductor.

## 2.3 Available measuring instruments on the Market

Before proceeding with the different concept boards, several available measuring instruments have been analyzed and compared. In the market there were different models and different technologies, that promised great results. Most solutions are based on shunt resistors or Hall sensor technologies.
This activity aimed to understand, if a technology that could satisfy the testing environment requirements already existed. In addition, it was a starting point from which to take inspiration, in this way it was possible to study and optimize already existing configurations.

In the following the list of the analyzed solutions.

- **dSPACE EV1025-04 board:** This component was already employed in the company. It is able to sense current on three different channels through three different Hall sensors, produced by LEM. Moreover, in order to meet different needs, it has the possibility to be completely configured by replacing the Hall sensor transducers. To increase the sensitivity of the EV1025 Current Measurement Board, it is possible to wind multiple loops through the LEM current transducer. The output of the board is an analog voltage. [11]

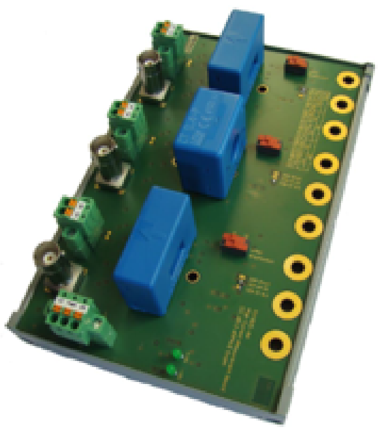

**Figure 2.15:** dSPACE EV1025-04 board

- **DMM7510 Multimeter:** This is a typical auto-ranged multimeter, the structure needed to measure the current was composed by several shunt resistors. It holds a very high accuracy, this peculiarity gives the possibility to measure the sleep current without any problem, with a very high reliability.

Besides the output display, it has different connectivity options such USB and LAN interface. [12]

**Figure 2.16:** DMM7510

- **imc CANSAS-IHR:** This solution is specifically designed for automotive utilization, especially to monitor the current, in the different states that can assume the control units in several operational conditions. It is made up by the series of two shunt resistors and by a power switch required to short-circuit one resistor when current increases. It has a very simple switching control circuit, where only the power switch has to be controlled. Output is provided via CAN bus with selectable data output rates. [13]

**Figure 2.17:** imc CANSAS-IHR

- **Joulescope JS110:** This is a precise DC energy analyzer designed for automotive applications, thus it is able to sense very low currents, up to the sleep current range (in the order of 50 $\mu$A). The current monitoring circuit is composed by seven different shunt resistors. The large number of resistors allows to minimize the induced burden voltage in each operating range. In this case, the output is only via USB, consequently it needs the specific proprietary software for computer connectivity. [14]


**Figure 2.18:** Joulescope JS110

- **VT7001A VECTOR and PXI-4065:** These two solutions have been taken in consideration since they were already employed in the company. They are integrated solutions respectively for CANoe and LABview. In the datasheet no information are provided concerning the transducers used.

**Figure 2.19:** VT7001A VECTOR and PXI-4065 [15] [16]

In conclusion, comparing and analysing in detail all the different solutions, each device could not completely meet the requirements (complete explanation of the requirements in chapter 4).
In the case of the dSPACE board, the main problem was related to the sleep current monitoring. This drawback could not be eliminated even by replacing the Hall sensors, since a transducer able to sense such low currents did not exist. In addition, it was not equipped with a CAN communication interface.
Regarding the digital multimeter, it could amply meet the accuracy requirements, but also in this case there was not the possibility to integrate the device in the testing equipment via CAN bus.
The IMC CANSAS-IHR was the best candidate for the current monitoring of the control units, since it was able to cover the entire current range. Besides this, it

is equipped with CAN communication interface and it had also the possibility to synchronize with the testing environment. However the main problems are related to the very high cost and the limited number of channels.
The Joulescope is also a very reliable solution, although it is not possible to integrate it via CAN with the testing equipment, but only through its proprietary software via serial communication.
Lastly the PXI-4065 and VT7001 were not able to be employed in other testing equipment except those they are designed for (e.g. PXI or VT system).

This leads to designing and building a custom solution, which can satisfy all the requirements, aiming a trade-off between accuracy, costs and circuitry simplicity.

# Chapter 3

# Requirements

## 3.1 Parameters choice

To design and engineer the whole instrument, the first step was the choice of the requirements, depending on these parameters it has been made the full design. Different measurements have been made through the Keysight InfiniiVision DS0X3034A oscilloscope associated with the Keysight N2822A 20 mΩ shunt resistor. This was done to understand the amount of current that flowing through the infotainment control unit. ECU has several number of states, which are linked with various operations such as: Calling operation, Bluetooth connection, upgrade loading, standby or sleep mode. Depending on the operation type the current could increase or decrease. In the following figures are shown different working operations.

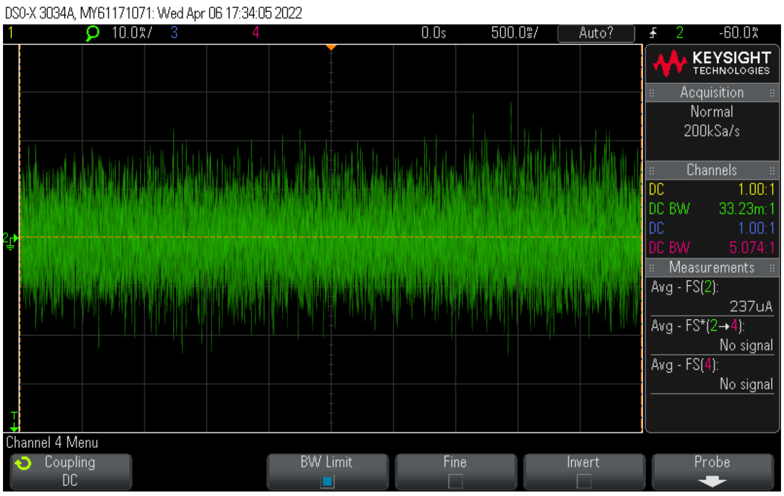


**Figure 3.1:** Current drains in MMI Sleep mode

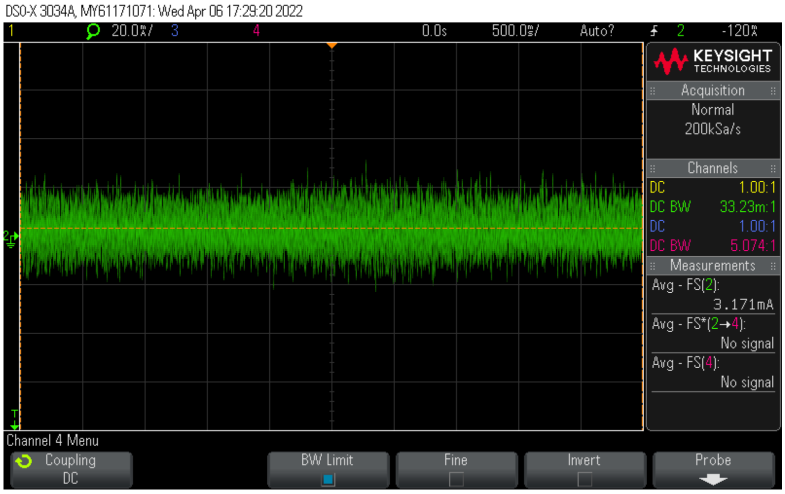


**Figure 3.2:** Current drains in MMI Stand-by

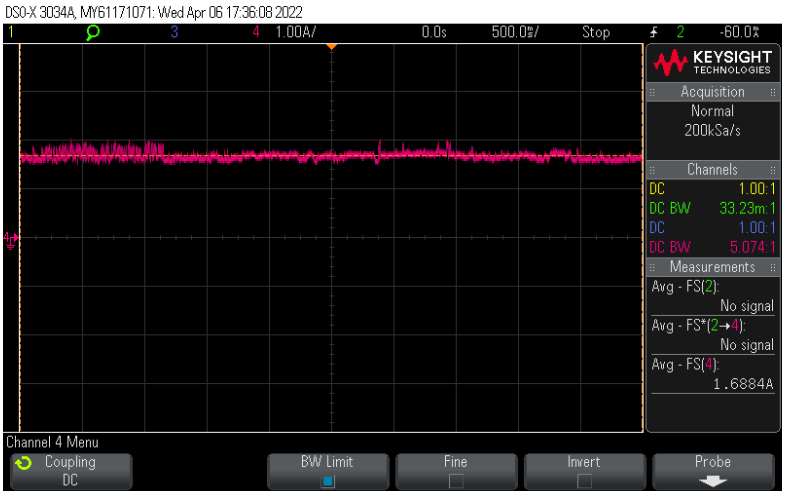


**Figure 3.3:** Current drains in MMI ON

It is possible to notice from the upper screen-shoots taken from the oscilloscope the 3 separate states of the current level: sleep mode, stand-by and as last the normal operation.
In the first state the current is very low approximately below 500 µA, it corresponds to the infotainment shut down state (sleep mode), the control unit enters in this configuration only after a predefined timer.
In the second state the current is in the milliampere order, the system is not completely turned off, it is waiting for a new command.
In the third state the current is over 1 A, it corresponds to the normal operation

conditions of the system, changing the operation type the current remains anyway around this value.

## 3.2 Parameters

**Current type:** The current required by the infotainment control unit is only DC type, so all the components will support only this type of current.

**Range:** Talking about the range, even if the infotainment control unit has several states dependent on the different operations. From the point of view of the measurement unit they can be summed up in only 3 states: sleep mode, stand-by and normal operation. For the lower limit it has been chosen 50 µA due to the low current in sleep mode; For the upper limit it has been chosen 10A, with this limit the instrument could monitor also different control unit respect to the one where the measurements were taken.

**Auto-ranged capability:** This is not properly a parameter but it is a property that the instrument must have, it means that the instrument can switch automatically between the high current range and the low current range, without external intervention. It will be addressed in the next chapters.

**Sensitivity:** This parameter is not constant but it will be dependent on the considered range, when the instrument handles low currents such the ones in sleep mode, the sensitivity will be 50 µA while for the high currents the sensitivity will be higher approximately 100mA.

**Output data frequency:** This parameter is related to the output data frequency of the instrument. The instrument will average the acquired data in order to reduce the noise in the final measurement.

**Output type:** The main output of the instrument will be via CAN, however it will also be implemented a little display. Thus in case of CAN bus failure, the current could be kept anyway under control. During the design phase it has been used the Serial output of Arduino.

**Multichannel capability:** Inside the testing environment are present more than one control unit, the instrument should be able to monitor 4 different current measurements.

**Burden Voltage:** This parameter is related to the voltage drop induced by current flowing through a resistor, since the device will use a shunt resistor for the low currents range, the instrument will be designed to not overcome the imposed limit of 0,1V. The power supply can monitor and manage only the voltage across the main control unit, increasing the burden voltage, will increase also the voltage drop across the remaining control units.

**Supply voltage:** The whole instrument will be powered at 12V, using the same voltage of the testing environment. If other voltage levels will be required, a voltage regulator will be designed inside the device.

**Synchronization:** As a key feature the instrument should be able to synchronize the measure read with the final output, obtaining a perfect timing between the testing environment and the monitor device.

**Localization in the circuit:** There exist different positions where the instrument can be insert:

- *Low side:* In this case, since in the testing environment the same GND can be shared between different ECUs, it is not possible to insert the instrument between the load and the ground. Placing the measurement device Low side, could generate some alternative current paths with lower impedance, consequently the current is not correctly measured by the instrument. (figure 3.4)

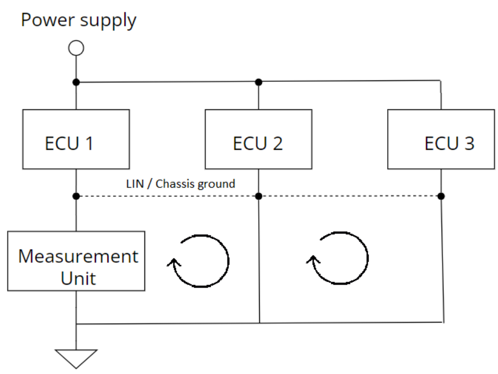


**Figure 3.4:** Low side simplified scheme

- *Power supply control loop:* In this configuration the instrument is directly inserted in the loop of the power supply unit. But since the power supply feeds also other control units and devices of the testing environment, it is not possible to use this method (fig 3.5). Otherwise instead of measuring the current flowing through the Infotainment ECU, it would be measured the sum of all the currents.

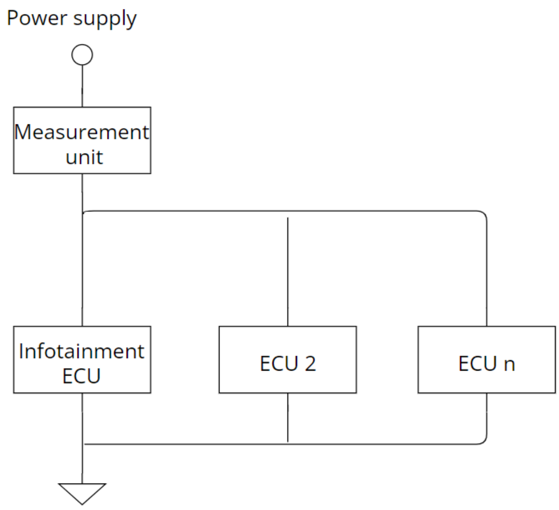


**Figure 3.5:** Power supply loop simplified scheme

- *High Side:* The instrument is inserted between the power supply and the load. Since one of the measurement unit pin is directly linked with the power supply voltage, specific sensing component are required, able to work with high common mode voltage ($\approx 30V$).
  For the application of this project, it has been chosen this localization type since the others two are not allowed.

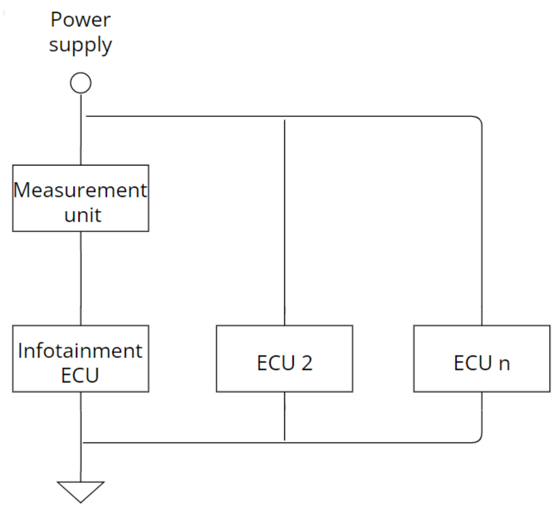


**Figure 3.6:** High side simplified scheme

## 3.3 Parameters resume

Following the table to group all the described parameters.

| Parameters | |
|---|---|
| Current type | DC current |
| Range | from 50 µA up to 10 A |
| Auto-ranged capability | Automatically switching between the 2 ranges |
| Sensitivity | 50 µA (low currents range) - 100 mA (high current range) |
| Output data frequency | 20 Hz |
| Output type | CAN / OLED display / Serial |
| Multichannel capability | 4 different channels |
| Burden voltage | 0.1 V |
| Supply voltage | 12 V |
| Synchronization | Timing between testing environment and monitor device |
| Localization | HIGH SIDE |

**Table 3.1:** Parameters resume

# Chapter 4

# Concept development

## 4.1 Introduction

To achieve the final electrical circuit, it was followed a lowercase procedure where different steps and hypothesis have been done. Through the initial research, different methods for current measuring have been deepened. In this phase, having at our disposal different techniques, it was not so trivial to find the right method.

The monitoring device is mainly composed by three distinct parts:

- *Main processing unit:* it is responsible of the tasks management, such as the control of the switches, the sensor readings and the communication with the external equipment.
- *Current sensor:* they are responsible of the current measure. Depending on the technologies, monitoring devices or external acquisition system may be required.
- *Switches:* these devices are necessary for the control and safeguard of the instrument.

Taking into account the required computational power and thanks to the company availability, Arduino has been chosen as the **Main processing unit** of the device. The **current sensor type** and the **switches type** have been chosen after a preliminary step-by-step phase. Subsequently all the steps will be described.

As first approach, it has been considered the design of a multi-range multi-meter, through this it was possible to understand the working principle of a device composed by more than one current transducer, in this case more than one shunt resistor.

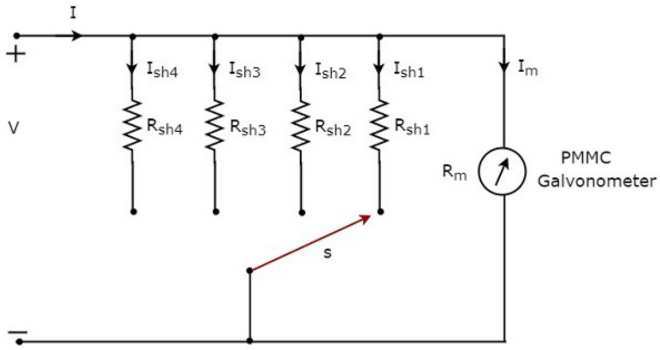


**Figure 4.1:** Multi-range ammeter

In the upper figure it is shown the simplified schematic of a device composed by four different shunt resistors. Depending on the current level, the internal micro-controller can switch between the different resistors. As mentioned above, the current is measured in function of the voltage drop across the resistor. Increasing the current intensity, in order to maintain the induced voltage across the resistor below a certain limit, the main processing unit has to proportionally decrease the resistor value.
For the complete design of a multi range current meter, different parameters have to be considered such as the maximum burden voltage, the maximum current limits, the sensitivity of the acquisition system and the resistor power dissipation.

**Sizing of a shunt resistor**
The two primary factors that need to be taken into account in calculating the shunt resistor value are two: the required accuracy at minimum load current and the power dissipation at maximum load current.
Considering the first factor mentioned above, it is important to take in consideration the minimum input offset voltage ($V_{OS}$) of the sensing device. The influence of this parameter is larger at low current, and it decreases with the increment of the sensed voltage. The relative offset error $e_{VOS}$ is calculated as in the equation 4.1.

$$e_{VOS} = \frac{V_{OS}}{V_{SENSE}} \cdot 100 \tag{4.1}$$

It is possible to notice that the error decreases with the increment of $V_{SENSE}$. In order to overcome the influence of this parameter, it has to be chosen a shunt resistor value that allows a minimum $V_{SENSE}$ much larger than $V_{OS}$.
The second factor is the power dissipation, the effect of this factor is the exact opposite of the previous one. If the current flow increases, the power dissipation increases (equation 4.2).

$$P_{max} = RI^2 \tag{4.2}$$

To handle with these two factors, it has to be found a sort of trade-off.
Besides the previous parameters, in the choice of the correct value of the shunt resistor, other three parameters have to be considered: the maximum current to be measured, the gain and the output voltage range $V_{OUT}$ of the sensing device.

$$R_{SHUNT} = \frac{V_{OUT}}{I_{MAX}} \cdot \frac{1}{Gain} \tag{4.3}$$

The last parameter to take into account is the burden voltage induced by the current flowing. It can not overcome the predefined limits.

$$V_{BURDEN} = R_{SHUNT} \cdot I_{MAX} \tag{4.4}$$

In order to choose properly all the resistors that make up the instrument, the 4 passages have to be done for all the ranges of the instrument.

**Choice of the Hall-effect sensor**
The choice of the appropriate hall sensor depends on the type of current, on the mounting type, on the power supply and on the current flowing.

In the following sections will be explained all the different attempts, before reaching the final design.

## 4.2 Shunt resistors design (First Attempt)

The first design was based only on the shunt resistor technology, anyway one of the main problems in a multi range device is related to the control of the "switches" needed to create an open or short circuit across the resistor not used. In this case, it has been taken inspiration from one of the commercial solutions mentioned in the chapter 2, the IMC Cansas. It is made up by only two shunt resistors and only one switch to measure a wide range of current (figure 4.2).

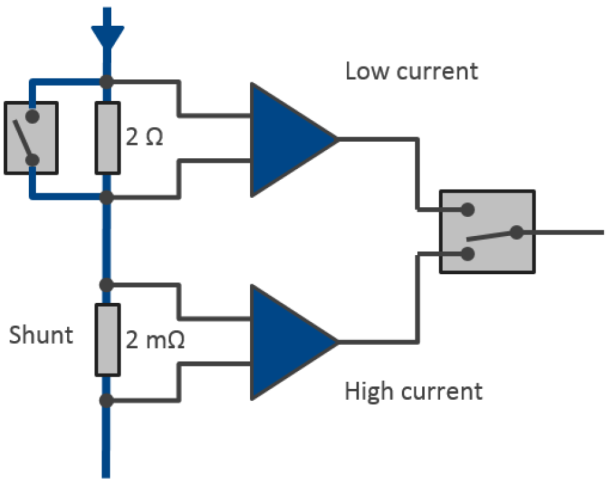


**Figure 4.2:** IMC Cansas simplified schematic

Thus, the first trial design was based on this simple schematic, in this way it is possible to cover the requested range of current, measuring the voltage drop across only 2 resistors, hence simplifying the switching control logic.
For reading the voltage across the two resistors, it has been chosen the INA225, a current-shunt monitor device from the TI company. In particular this component has an output voltage depending on the current level, a wide common-mode range: 0 V to 36 V, a maximum offset voltage of ±150 µV and the possibility to set 4 different gains (25, 50, 100, 200). Thanks to the high common mode voltage is possible to place this device between the power supply and the load, HIGH SIDE. In the figure 4.3 it is shown the first simplified circuit created with LTspice.

For sizing the resistor a simple procedure was followed, it has been taken in consideration especially two different parameters: the required accuracy at minimum load current and the power dissipation at maximum load current. Higher will be the voltage across the resistor and larger will be the accuracy in the low current range. The gain was set equal to 25.

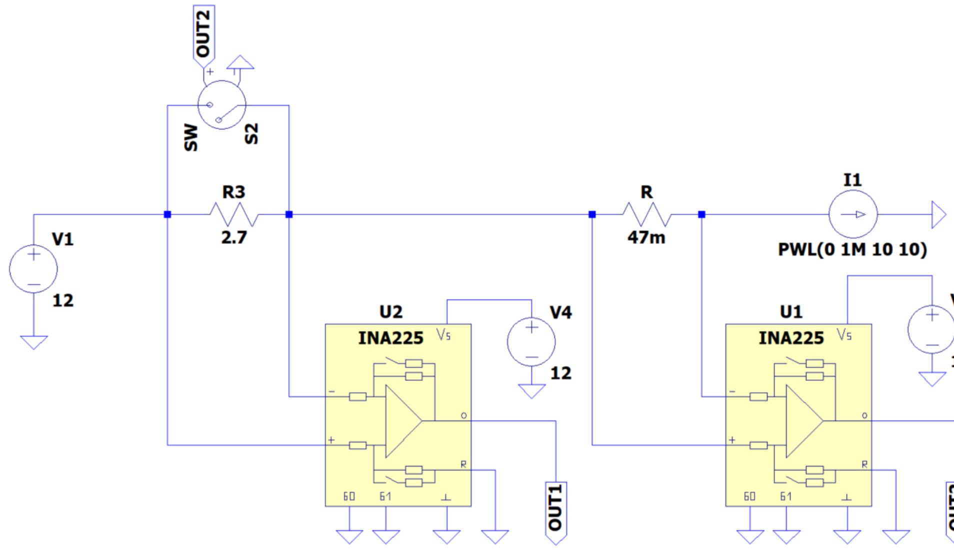


**Figure 4.3:** First trial: LTspice circuit

In the following, the procedure used for the resistor sizing, to obtain a resistance value as high as possible, it has been considered only the maximum flowing current and the maximum supply voltage for the INA225:

- *Low current resistor:* it is responsible of the low current range, from 50 µA up to 200 mA.

$$R_3 = \frac{Vd}{G}\frac{1}{I_l} = \frac{12\,\mathrm{V}}{25}\frac{1}{200\,\mathrm{mA}} = 2.4\,\Omega \approx 2.7\,\Omega \tag{4.5}$$

  $V_d$ is the desired output voltage, successively acquired by the acquisition system. $G$ is the set gain of the current monitor, 25 in this case. $I_l$ is the upper current limit, which corresponds to 200 mA. The final result has been approximated to the closest E12 series resistor value.

- *High current resistor:* it is responsible of the high current range, from 200 mA up to 10 A.

$$R = \frac{12\,\mathrm{V}}{25}\frac{1}{10\,\mathrm{A}} = 48 \times 10^{-3}\,\Omega \approx 47 \times 10^{-3}\,\Omega \tag{4.6}$$

  As for the previous case, the gain is set equal to 25 and $I_l$ is set equal to the upper current limit, 10 A. Also in this case the final result is approximated to the closest E12 series value.

Below it is explained the working principle:

- *Low current range:* overcoming the imposed upper limit of 200 mA, the switch closes immediately and creates a short circuit over the resistor on the left, in order to deflect the current onto itself and proceeding with the measure through the second resistor.

- *High current range:* the second resistor is constantly active, it does not need a switch that can deflect the current flow, since it should be able to dissipate the requested amount of power.

To simulate the circuit operation it was used a 12 V DC power supply as battery imitation; and in order to emulate the ECUs working, a current power supply with a linear current increment, ranging from 0 A up to 10 A.
In this configuration the Arduino ADC was supposed to be able to read the output voltage coming from the INA225, and after processing the data can return the current value.
In the figure 4.4 it is shown the simulated characteristic of the device, where it is possible to understand the performance of the circuit. The two lines correspond to the output of the two different INA225. The green one corresponds to the voltage-output characteristic of the INA225 assigned for the low current measurement, overcoming the upper limit of 200 mA the switch closes and consequently the corresponding INA measures 0 V. The blue one corresponds to the voltage-output characteristic of the INA225 assigned for the measure of the high current range, which is constantly growing. The two ideal characteristics are linear up to their limits.

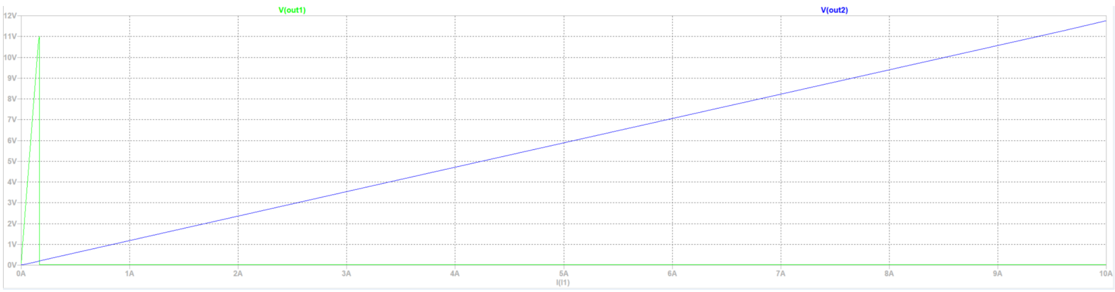


**Figure 4.4:** First trial: Output Characteristic

This configuration has been discarded for several reasons:

- *Offset voltage limits:* Measuring 50 µA, with a 2.7 Ω resistor, the corresponding sensed voltage is 135 µV. As a consequence this error is too high.

$$e_{VOS} = \frac{V_{OS}}{V_{SENSE}} \cdot 100 = \frac{150\,\mu\text{V}}{135\,\mu\text{V}} \cdot 100 = 111\% \tag{4.7}$$

- *Resolution of Arduino ADC:* Measuring very low currents is required a very high resolution from the Arduino ADC, but having only 10 bit referred to a voltage of 5 V, it can cover only 1023 values with a resolution of 4.9 mV that is not enough for this purpose.

$$ADCresolution = \frac{V_{REF}}{2^n} = \frac{5\,\mathrm{V}}{1024} = 4.9\,\mathrm{mV} \tag{4.8}$$

  As it can be seen, ideally Arduino can detect a minimum voltage drop coming from the INA225 equal to 4.9 mV. Consequently applying the formula 4.9, the minimum detectable current by the Arduino ADC is 72.6 µA, which is not enough for the sleep currents sensing (Sleep current $\approx$ 50 µA). It has to be taken into account that usually, it is necessary to stand at least 3 times the minimum step size value.

$$I_{min} = \frac{V_{LSB}}{G \cdot R} = \frac{4.9\,\mathrm{mV}}{25 \cdot 2.7\,\Omega} = 72.6\,\mu\mathrm{A} \tag{4.9}$$

- *Maximum ADC voltage input limit:* INA225 has a tunable gain, but even using the lowest gain (G=25), the maximum input voltage limit of the Arduino ADC of 5 V is exceeded. Considering the low current resistor, it would be possible to move to the higher resistor range as soon as the limit of the ADC is reached but anyway, it is not feasible stay within the ADC limit for the high current resistor. It would be necessary to scale the voltage value using a voltage divider, but the accuracy would be greatly decreased.

- *Component shortage:* Since at the beginning of the project there was a strong lack of electronic devices due to the Coronavirus pandemic, some of the components were difficult to find, such as the INA225.

- *Power dissipation:* Besides the current limits and the burden voltage, it is important to ensure that the power dissipation is adequate.
  In the low current resistor, applying the following formula:

$$P = R \cdot I^2 = 2.7\,\Omega \cdot (200\,\mathrm{mA})^2 = 0.108\,\mathrm{W} \tag{4.10}$$

  It is not a problem to find a shunt resistor able to dissipate this amount of power, however it is not the same regarding the second current range.

$$P = R \cdot I^2 = 47\,\mathrm{m}\Omega \cdot (10\,\mathrm{A})^2 = 4.7\,\mathrm{W} \tag{4.11}$$

  This second amount of power is relatively high and it requires specific power shunt resistors.

- *Burden Voltage:* In both case the induced voltage drop across the shunt resistors is relatively high and overcomes the predefined requirement (0.1 V).

$$V_B = R \cdot I_{MAX} = 2.7\,\Omega \cdot 200\,\text{mA} = 0.54\,\text{V} \tag{4.12}$$

$$V_B = R \cdot I_{MAX} = 47\,\text{m}\Omega \cdot 10\,\text{A} = 0.47\,\text{V} \tag{4.13}$$

## 4.3 Hall-effect sensors design (Second Attempt)

This second trial has been done only using hall sensor transducers technologies, there are many advantages using this configuration. Firstly by using hall sensors, there is no need to insert external components in the circuit. Secondly, thanks to the hall sensors performance each transducer supports higher currents respect to the nominal one, hence the switches are not required for shorting the transducers not used.
In the figure 4.5 it is shown the second simplified circuit created with LTspice.

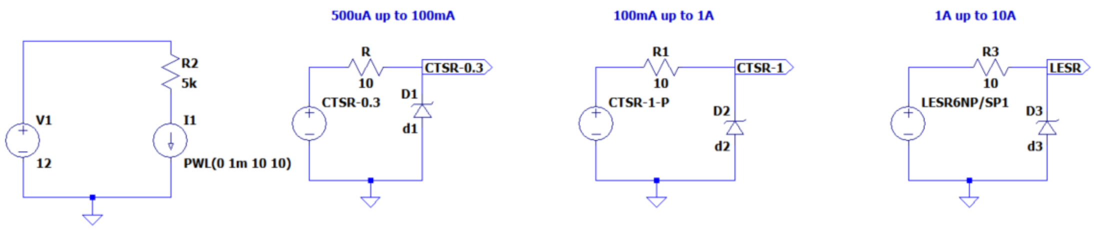


**Figure 4.5:** Second trial: LTspice circuit

The main high voltage circuit is composed by a 12 V DC power supply as imitation of the battery, a resistor and lastly as in the previous case a current power supply needs to simulate the ECU behavior. The current power supply generates a linear increment to cover the complete range of working.
Since the custom libraries of these hall sensor transducer do not exist, for reproducing the Hall sensor characteristic, it has been used a simple circuit composed by a custom voltage power supply, a resistor and a zener diode. The custom voltage power supply generates the voltage in function of the current that flows inside the resistor R2, placed in the main circuit, in addiction a white noise was added to reproduce the hall sensor output noise.

Ideally in the main circuit are included 3 different hall effect transducers manufactured by the LEM company (table 4.1):

| Name | Theoretical Sensitivity [V/A] | Nominal current [mA] | Theoretical Range |
|---|---|---|---|
| **CTSR 0.3-P** | 4 | 300 | $100\,\mu A \div 100\,mA$ |
| **CTSR 1-P** | 1.2 | 1000 | $100\,mA \div 1\,A$ |
| **LESR 6-NP** | 0.1042 | 6000 | $1\,A \div 10\,A$ |

**Table 4.1:** Hall sensors current transducers

The three different Hall sensors have been chosen considering different factors: the maximum primary current for each transducer, the supply voltage (5 V), the sensitivity, the output noise and the possibility to PCB mounting.
Using 3 different sensors it is possible to cover the full current range, but it is required to increase the resolution in the low current range or it is impossible to reach up to 50 µA.
Ideally, a technique to increase the sensitivity of the hall sensor is to wind the wire around the primary circuit, obtaining that the resulting sensitivity will be the multiplication of the winding number times the nominal sensitivity.
Consequently, the voltage-output of the 3 sensors are read by the Arduino ADC.
In the figure 4.6 it is shown the output of the 3 sensors:

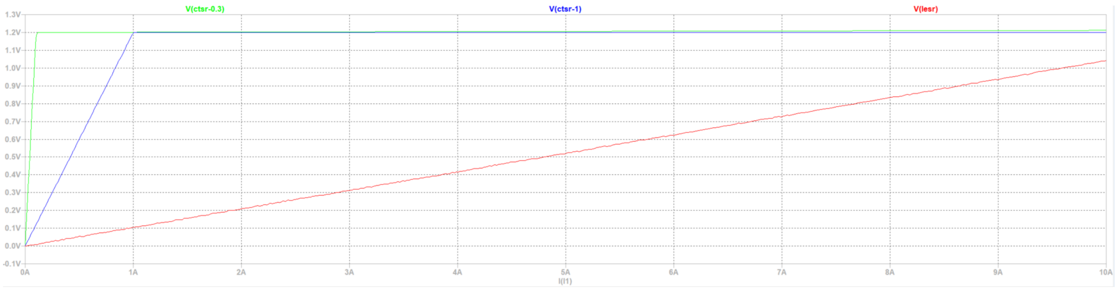


**Figure 4.6:** Second trial: Output Characteristic

In this case it has been supposed that for the low current range employing the CTSR 0.3-P, by winding three times the wire around the primary circuit, it was possible to reach a sensitivity of 12 V/A, hence with a current drains of 50 µA, the hall transducer can generate an output equal to 0.6 mV (equation 4.14).

$$V_{out} = S \cdot I = 12\,\mathrm{V/A} \cdot 50\,\mu\mathrm{A} = 0.6\,\mathrm{mV} \tag{4.14}$$

Where $S$ is the ideal sensitivity of the instrument and I is the current considered.
In addition to the increasing of the sensitivity, it is also necessary to consider the

reduction in the maximum measuring current range. As in the formula (4.15):

$$I_{MAX} = \frac{I_{PRM}}{N_w} = \frac{500\,\text{mA}}{3} = 166.67\,\text{mA} \tag{4.15}$$

Also the "new" maximum current range meets the requirements, since the CTSR 0.3-P has to measure a current up to 100 mA.

In the case of the other two hall sensors, it was not required to increase the nominal sensitivity with multiple windings.
CTSR 1-P voltage output:

$$V_{out} = S \cdot I = 1.2\,\text{V/A} \cdot 100\,\text{mA} = 120\,\text{mV} \tag{4.16}$$

$$V_{out} = S \cdot I = 1.2\,\text{V/A} \cdot 1\,\text{A} = 1.2\,\text{V} \tag{4.17}$$

LESR 6-NP voltage output:

$$V_{out} = S \cdot I = 104.2\,\text{mV/A} \cdot 1\,\text{A} = 104.2\,\text{mV} \tag{4.18}$$

$$V_{out} = S \cdot I = 104.2\,\text{mV/A} \cdot 10\,\text{A} = 1.042\,\text{V} \tag{4.19}$$

As it can be seen the output range of the two sensors respect the Arduino ADC voltage input, hence it is not required any further improvement of their sensitivity. This configuration has been discarded for several reasons:

- *Resolution of Arduino ADC:* It is required a very high resolution from the acquisition system, for measuring very low current. However, as in the previous attempt, Arduino has ideally a resolution equal to 4.9 mV that is not enough for this purpose, since it cannot sense the sleep current (Sleep current ≈ 50 µA). The minimum detectable current should be:

$$I_{id,min} = \frac{4.9\,\text{mV}}{12\,\text{V/A}} = 408.33\,\mu\text{A} \tag{4.20}$$

- *ADC number pins:* each LEM sensor has two different outputs, besides the one dependent on the current measured, there is a second output that is called Voltage reference ($V_{REF}$), it provides a constant voltage. To obtain the final current measurement, it is required to take in consideration both signals, consequentially each transducer needs 2 different pins of the Arduino ADC. In the case of device able to sense on four different channels, the number of ADC pins is not enough. In the figure (4.7) it is shown a simplified electrical scheme of the hall transducer, provided by the LEM company.

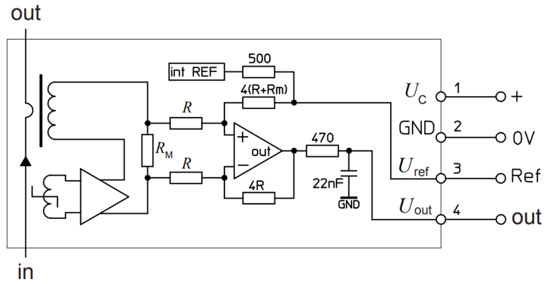


**Figure 4.7:** LEM transducer electrical scheme

- *Output noise:* In the datasheet of each component is provided the amount of noise produced by the voltage-output of the hall transducer. In the case of the CTSR-0.3-P it is equal to 6 mV, this value will be tripled due to the three windings around the primary circuit. In this way having 18 mV as white noise, this means to have an uncertainly of 1.5 mA (equation 4.21). This value is not acceptable for measuring sleep currents.

$$e = \frac{Outputnoise}{Sensitivity} = \frac{18\,\mathrm{mV}}{12\,\mathrm{V/A}} = \pm 1.5\,\mathrm{mA} \tag{4.21}$$

  Instead for the other two transducers, thanks to the higher current ranges, this error is negligible since, by applying the formula (4.21) it is respectively $\pm$ 5 mA for the CTSR-1P and $\pm$ 95 mA for the LESR 6-NP.

- *Considerable footprint:* each sensor requests a large amount of space, the CTSR 0.3-P and CTSR 1-p have the same size 44,6x45x17,9mm , instead the LESR-6P is 20,03x21,9x13,4mm.
  In the case of multiple sensors and multiple channels considering the final circuit composed by all the footprints, the resulting space is huge. Since the instrument should be inserted in the testing environment, it cannot take up a significant amount of space.

## 4.4 Sensor fusion design (Third Attempt)

Starting from the two previous cases, it has been designed a sensor fusion configuration, in order to obtain a circuit that could fit the requirements. In this way, it is possible to take advantage by the two different characteristics of the two different sensor types. It is quite straightforward to understand that the shunt resistor works better in the low range of currents and the hall sensor is easily implemented for measuring the high currents range, this trial started from this statement.

In the circuit (fig 4.8) it is shown the resulting merging of the two previous trials, which is ideally able to cover the required range of currents.

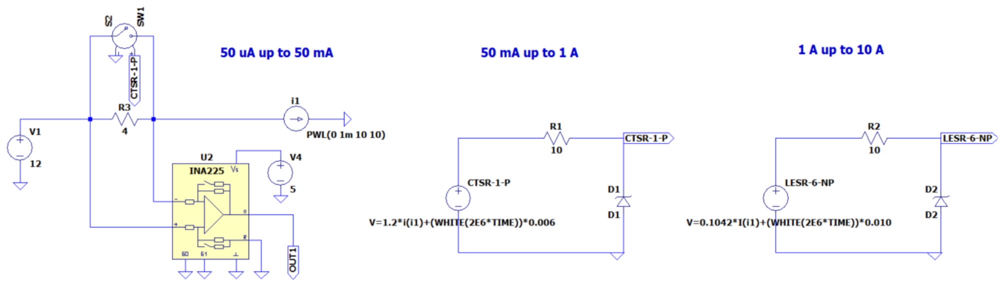


**Figure 4.8:** Third trial: LTspice circuit

Also in this case the main circuit is always composed by a 12 V DC power supply as imitation of the battery and by a current power supply that simulate a linear current increment, in order to cover the whole range.
The measurement device is composed by three different transducers: one shunt resistor, need to cover with an high accuracy the low current range and two hall sensors to cover the high current range. INA225 is the responsible for sensing the voltage drop across the shunt resistor, it generates a voltage-output acquired by Arduino ADC that will be processed to obtain the current intensity, the same happens for the voltage-output of the hall sensors. As it can be seen the shunt resistors will be short-circuited by using a single switch, as in the first attempt.

Design phase:

- *Low current range:* It is referred to the current range between 50 µA and 50 mA. In this attempt it has been tried to maximize the value of the resistance, in order to obtain an output voltage coming from the INA225, readable by the Arduino ADC during the sleep current operational conditions. This is done using the minimum INA225 gain, equal to 25.

$$R = \frac{V_{ADC}}{G}\frac{1}{I_{MAX}} = \frac{5\,\text{V}}{25}\frac{1}{50\,\text{mA}} = 4\,\Omega \tag{4.22}$$

  $V_{ADC}$ is chosen equal to 5 V in order to respect the limit imposed by the Arduino ADC. $I_{MAX}$ is equal to 50 mA, the upper limit chosen for this range. With these values, it has been found a resistor value equal to 4 Ω. In this way the induced voltage drop in the sleep current range is equal to:

$$V_{INA225} = R \cdot I_{MIN} \cdot G = 4\,\Omega \cdot 50\,\mu\text{A} \cdot 25 = 5\,\text{mV} \tag{4.23}$$

In this case the minimum voltage generated by the INA225 is almost equal to the Arduino ADC sensitivity ($\approx 4.9\,\mathrm{mV}$).

- *Switching logic:* This is done by using a switch that is driven by the voltage coming from the CTSR-1-P. This is the true advantage of using a sensor fusion device, because it is possible to overlap the range between the shunt resistor and the hall sensor. This key feature is made possible by the fact, that the hall effect sensor is constantly active. At 50 mA it generates a voltage equal to 60 mV (formula 4.24).

$$V_{CTSR1-P} = S \cdot I = 1.2\,\mathrm{V/A} \cdot 50\,\mathrm{mA} = 60\,\mathrm{mV} \tag{4.24}$$

  The voltage coming from the CTSR 1-P is perfectly detectable by the Arduino ADC, since it is much more higher than its sensitivity of 4.9 mV. In this way overcoming 50 mA the switch will be immediately closed.
  Moreover since both hall sensors can withstand a current flow much higher than the predefined limit ([17] [18]), they do not require any protection switch.

- *High current range:* This range is divided in two different different intervals: one assigned to the CTSR 1-P between 50 mA and 1 A; the second one assigned to the LESR 6-NP between 1 A and 10 A.

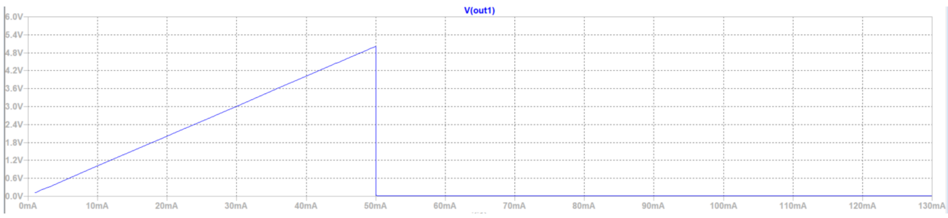


**Figure 4.9:** Third trial: LTspice Low current range characteristic

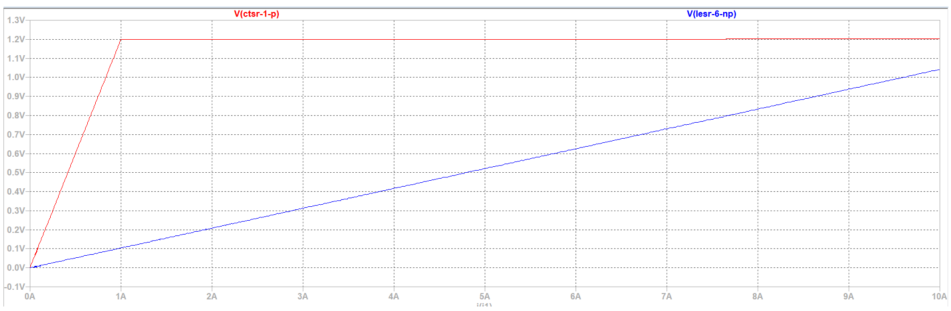


**Figure 4.10:** Third trial: LTspice High current range characteristic

In the figure (4.9 and 4.10) are shown the three output characteristics, they were separated in two different diagrams for a better understanding of the small current range. The first image is related to the two INA225 output between 50 µA up to 130 mA, instead the second image is related to the output of the two hall sensors from 50 mA up to 10 A .
In this case the two problems related to the acquisition system have been solved: the first, related to the overcoming of the 5 V ADC input limits and the second, with the low resolution in the low current range.
The shunt resistor has to dissipate 0.01 W, with a current flow equal to 50 mA (equation 4.25).

$$P = R \cdot I^2 = 4 \cdot (50\,\text{mA})^2 = 0.01\,\text{W} \tag{4.25}$$

Anyway, this configuration still has some peculiarities to be improved:

- *Offset voltage limits:* Measuring 50 µA with a 4 Ω resistor, the corresponding sensed voltage is 200 µV. As a consequence this error is still too high.

$$e_{VOS} = \frac{V_{OS}}{V_{SENSE}} \cdot 100 = \frac{150\,\mu\text{V}}{200\,\mu\text{V}} \cdot 100 = 75\% \tag{4.26}$$

- *ADC number pins:* Besides the INA225 output, it has to be taken into account also the two outputs of each hall sensor. Since it was requested six different sensed pins, Arduino ADC is not enough.

- *Considerable footprint:* In the case of multichannel capability, the footprint is not negligible since the number of transducer is considerable.

- *Burden Voltage:* The induced burden voltage across the shunt resistor, when the current is equal to 50 mA, overcomes the imposed limit on the requirement.

$$V = R \cdot I = 4\,\Omega \cdot 50\,\text{mA} = 0.2\,\text{V} \tag{4.27}$$

  The imposed limit is 0.1 V.

- *ADC accuracy:* Altough the minimum voltage generated by the INA225 during the sleep current condition is almost equal to the Arduino ADC sensitivity, it is recommended to stay above at least three or four times the minimum step size of the ADC.

- *Lack of computational power:* In the case of multichannel capability there are several devices to manage, this decreases exponentially the sampling time.

## 4.5 Final design

### 4.5.1 Initial Concept

Starting from the sensor fusion idea of the third attempt, there were some problems to solve:

- **ADC pin number:** in the case of multichannel capability the resultant number of pin has to be lower or equal to the Arduino ADC number.
- **ADC voltage limitation:** Arduino ADC at maximum could sense up to 5 V, therefore the maximum drop across the resistor after the amplification stage, has to be lower than this upper limit. Regarding the minimum voltage, Arduino has a sensitivity ideally equal to 4,9 mV. Therefore, the output of any transducer has to be larger than two or three times the ideal sensitivity value aforementioned.
- **Switching logic:** due to the limited Arduino computational power, the switching logic has to be as simple as possible, also taking in consideration the multichannel capability.
- **Footprint sizing:** especially the hall sensor needs a considerable amount of space, as a consequence it is better to find a solution with a limited number of Hall sensors.

After extensive analysis since the problems were mainly given by the Arduino ADC, it has been found a substitute for the INA225 current monitor, the **INA226**.
This device belongs to the same family of components of the INA225, but with some key features that can solve some difficulties: the output is not in voltage but all the data are totally sent on I2C bus, as a consequence only 2 analog pins of the Arduino shield will be used; internally it has not a fixed gain but has a simple ultra precise 16 bit ADC. In this way it is possible to use a very small resistor value to sense very low currents, in this way the burden voltage across the shunt resistor will not be a problem.
Before to proceed, it has to be said that due to the shortage of the semiconductors given by the global pandemic, it was not possible to find the INA226 current shunt monitor alone (without the conditioning circuit). Moreover, since this current monitor satisfied all the requirements, it was chosen a plug and play PCB module (Arduino compatible), already provided with the conditioning circuit suggested by the manufacturer.
In the figure (4.11 and 4.12) it is shown the component and the corresponding electrical circuit.
As it can be noticed from the images, a shunt resistor equal to 100 mΩ is directly soldered on the circuit, consequentially the initial configuration was based on this

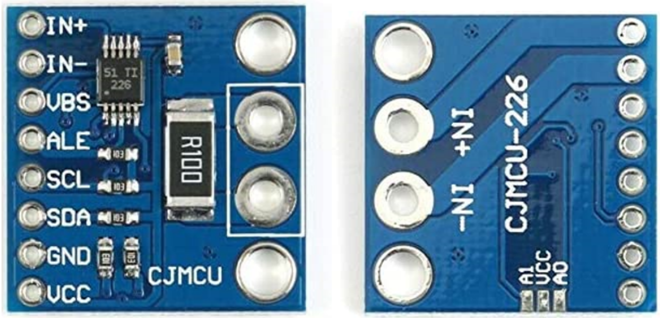


**Figure 4.11:** INA226 Back and Front

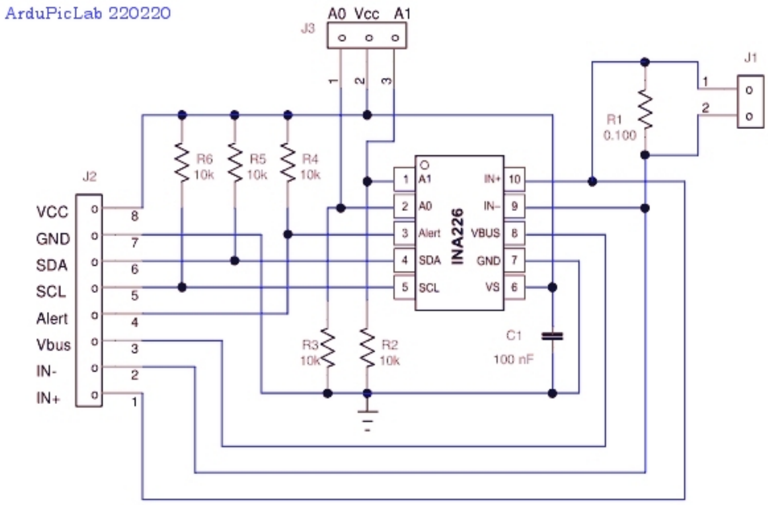


**Figure 4.12:** INA226 Electrical scheme [19]

shunt value.

Keeping in consideration the datasheet of the INA226 [20], the upper limit of the shunt voltage input range of the instrument is equal to 81.92 mV. As a consequence by applying the formula 4.28:

$$I_{MAX} = \frac{V}{R} = \frac{81.92\,\mathrm{mV}}{100\,\mathrm{m\Omega}} = 819.2\,\mathrm{mA} \tag{4.28}$$

The maximum current that can flow through the provided resistor is 819.2 mA, hence this shunt could cover a very large low current range. Thereafter, considering a sleep current of 50 µA, the resulting drop voltage across the resistor is 5 µV. The minimum voltage detectable by the INA226 corresponds to the internal ADC LSB step size, in this case it is equal to 2.5 µV. However, considering also the shunt offset voltage RTI (respect to the input) of the INA226, this value corresponds to $\pm 10\,\mu\mathrm{V}$. As a consequence, in the final design, to avoid inaccurate measures, it would be better to replace the $100\,\mathrm{m}\Omega$ shunt resistor with a larger value, that can ensure at least a minimum voltage drop across the shunt three or four times the shunt offset voltage RTI of the INA226.

To maintain the switching logic as simple as possible, it has been used one single switch, necessary to short circuit the shunt resistor just crossed the fixed low current range.

It has to be considered also the maximum current that can flow inside the provided shunt resistor, depending on the maximum allowed burden voltage:

$$I = \frac{BurdenVoltage}{R_{shunt}} = \frac{0.1\,\mathrm{V}}{100\,\mathrm{m}\Omega} = 1\,\mathrm{A} \tag{4.29}$$

Thanks to the fact that the induced burden voltage remains negligible up to 1 A (4.29). It has been possible to design a circuit composed by only 2 transducers, a shunt resistor for low currents, and one hall sensor, the LEM LESR 6-NP for the high currents range. The shunt resistor voltage will be monitored by the INA226 communicating with Arduino via i2c and the voltage-output of the hall transducer is sensed by the Arduino ADC. As mentioned above, using the LESR 6-NP, ideally it is possible to read low currents up to 47 mA (4.30).

$$I_{MIN} = \frac{S_A}{S_{LESR}} = \frac{4.9\,\mathrm{mV}}{104.2\,\mathrm{mV/A}} = 47\,\mathrm{mA} \tag{4.30}$$

$S_A$ is the ADC Arduino sensitivity and $S_{LESR}$ is the sensitivity of the LESR hall sensor.

Since the measurement through the provided shunt resistor can span ideally up to 800 mA and the Arduino ADC can read low current up to 47 mA, it is possible to largely overlap the two different measurements coming from the two transducers, in order to obtain a sensor fusion measurement. In addition, it is possible to take advantage from this principle by controlling the switch, using the measurement coming from the Hall Sensor. Following the simplified scheme fig 4.13.

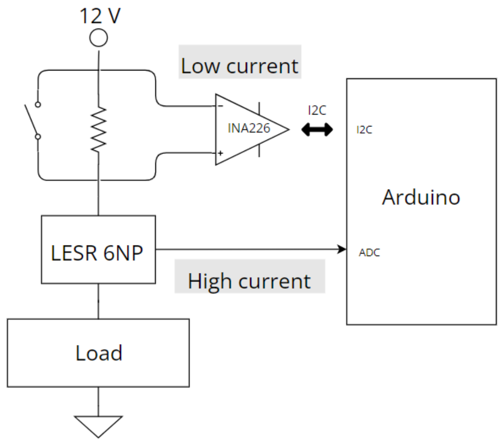


**Figure 4.13:** Simplified final concept scheme

In the next chapter will be deepened the final design development.

### 4.5.2 Development

Before to start with the final development, different steps have been made:

1. *Single component operational test:* each component was tested individually, to understand if the simulated behaviour was the same also in the testing environment. The tested components were: INA226 with the corresponding shunt resistor, Hall effect sensor and the switching logic.

2. *Arduino programming:* Talking about the software, before to merge all the various programs, also in this case each code has been tested individually.

3. *Breadboard testing:* Finally before to create the definitive prototype, all the different components have been tested on the breadboard, merging them in the final circuit using one single channel.

**INA226:** Firstly it was tested the current monitor device, to understand if it was able to sense very low currents. Since the component was sold without the connectors, the first step was to solder the PCB header. After that, to test the component it was required to create an Arduino program that was able to set all the device parameters and read the data on the I2C.
In the figure 4.14 it is shown the single component test on the breadboard.
For testing the component, it has been used a simple circuit composed by the power supply, Arduino, INA226, a trimmer and a resistor (figure 4.15).

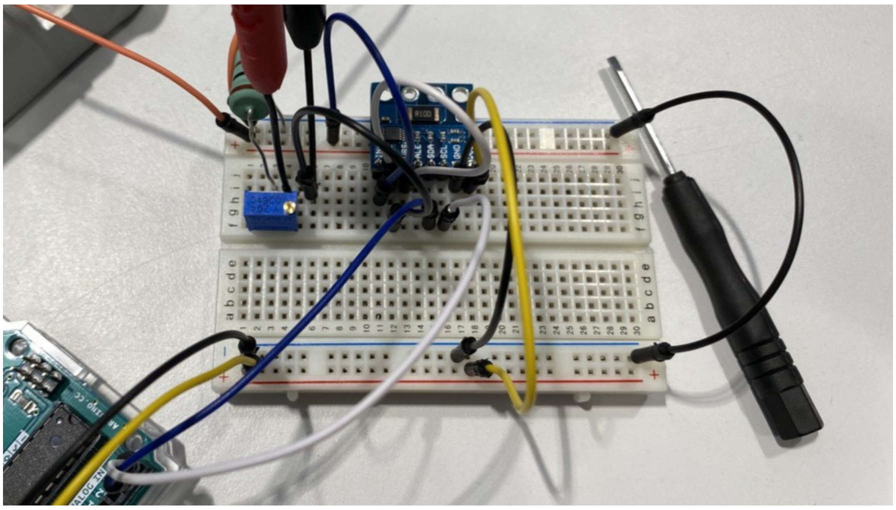

**Figure 4.14:** Bredboard testing: INA226 individual

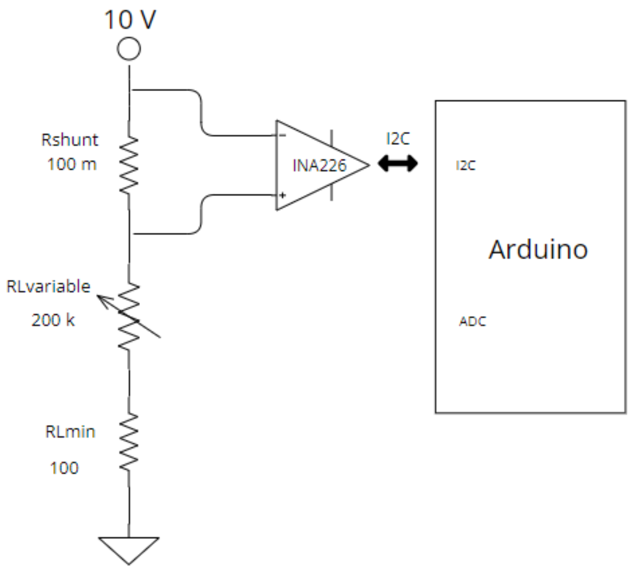


**Figure 4.15:** Bredboard testing: INA226 individual simplified electrical scheme

More in deep, for the breadboard testing for safety reason it has been designed a circuit powered by a 10 V power supply and a maximum current of 100 mA (4.31). This is done by using a resistor in series ($R_{L,MIN}$) to the 200 kΩ trimmer, which needs to maintain the current under the imposed limit, furthermore the trimmer was used to simulate the change of current inside the circuit.

$$I_{MAX} = \frac{V_{SUPPLY}}{R_{L,MIN}} = \frac{10\,\mathrm{V}}{100\,\Omega} = 100\,\mathrm{mA} \tag{4.31}$$

**INA226 programming** INA226 has 2 pins A0 and A1, which is possible to pull-UP or pull down-DOWN, the combination of the 2 pins needs to select one of the 16 addresses on the I2C bus. This peculiarity is very important for the multichannel capability, where on the same bus is present more than one current monitor device.
This device has two key features: the possibility to decide the conversion time and the possibility to average over a predefined value of samplings. It is possible to choose the conversion time between each sample, this value can range from 140 us up to 8.244 ms. In addition the component can also set the number of measurements to average, according to meet the requirements and to filter the noise.
Since on the web there are a lot of INA226 compatible libraries, after some trials it has been chosen the one that could fit better the company needs, practically the one with the highest sensibility, "High side monitor libraries" from LEAP, made by Paul Gallagher [21].
The library was lacking of the 2 functionalities regarding the possibility to set the conversion time and the averaging, they have been added in a second moment. Below it is represented the code regarding the 2 added functions.

```
// Averaging function
bool Ina226Driver::setAverage(uint8_t avg)
{
  if (avg > 7) return false;
  uint16_t mask = readRegister16(InaRegister::Configuration);
  mask &= 0xF1FF;
  mask |= (avg << 9);
  writeRegister16(InaRegister::Configuration, mask);
  return true;
}
uint8_t Ina226Driver::getAverage()
{
  uint16_t mask = readRegister16(InaRegister::Configuration);
  mask >>= 9;
  mask &= 7;
  return mask;
// Conversion time
bool Ina226Driver::setShuntVoltageConversionTime(uint8_t svct)
{
  if (svct > 7) return false;
```

```
  uint16_t mask = readRegister16(InaRegister::Configuration);
  mask &= 0xFFC7;
  mask |= (svct << 3);
  writeRegister16(InaRegister::Configuration, mask);
  return true;
}
uint8_t Ina226Driver::getShuntVoltageConversionTime()
{
  uint16_t mask = readRegister16(InaRegister::Configuration);
  mask >>= 3;
  mask &= 7;
  return mask;
}

    return M
```

As it can be seen each single feature is divided in 2 different functions, the first for setting and the second for returning the inserted value on the I2C.
After this small addition, it was developed the program for reading and processing the data on the I2C bus, it is reported below.

```
#include "Arduino.h"
#include "ina226_driver.h"
const float R_SHUNT      = 0.138034;  // nominally 0.100 ohm
const float MAX_BUS_AMPS = 0.8;
const uint32_t SERIAL_SPEED = 115200;
const uint8_t  INA_ADDR0 = 0x40;
Ina226Driver ina0 = Ina226Driver();
void setup() {
  ina0.begin(INA_ADDR0);
  ina0.calibrate(R_SHUNT, MAX_BUS_AMPS);
  ina0.setShuntVoltageConversionTime(1);
  ina0.setAverage(3);
}
void loop() {
  static char sprintfBuffer[15];
  static char current_mA0[15];
  dtostrf(ina0.readCurrent() * 1000.0 , 9, 3, current_mA0);
  sprintf(
    sprintfBuffer,
    "%smA\n",
    current_mA0,
  );
  Serial.print(sprintfBuffer);
  Serial.print(millis());
```

```
}
```

In the initial part of the program, the different parameters are set, this step required for the characterization of the device: the shunt value, the maximum expected current, the serial speed, the INA226 address and as last the conversion and averaging time. The final part is devoted firstly to the reading of the data and secondly to the printing on the serial monitor. For computing the sampling rate, millis is printed after each measurement, this value returns the value of milliseconds passed since the Arduino board began running the current program, the difference between two consecutive measurements gives the sampling rate.
As discussed before it was used the 100 mΩ shunt resistor already soldered on the PCB module, but after some comparisons with other measurement devices, this value was properly changed. Subsequently this little change of the resistor value, the low sensed currents were comparable to the oscilloscope measures up to 500 µA. This means that in the final design the shunt resistor value has to be properly increased.

**Hall Sensor:** Since the real sensitivity of the Arduino ADC was unknown, the first Hall-effect sensor tested was the one with the higher sensitivity [V/A], the LEM CTSR 1-P. Also in this case the testing circuit was simple (figure 4.17), composed only by the power supply, Arduino, the Hall sensor and a resistor that acted as a simulated load. Unlike the first case, to simulate the current variation it has been tuned the power supply voltage value, consequentially the current was imposed by the fixed power resistor (as it can be seen in the figure (4.16) the resistance was imposed by the parallel of several resistances, in order to dissipate the requested power). This was possible thanks to the fact that the hall sensor accepts a wide range of input voltage, without being damaged.

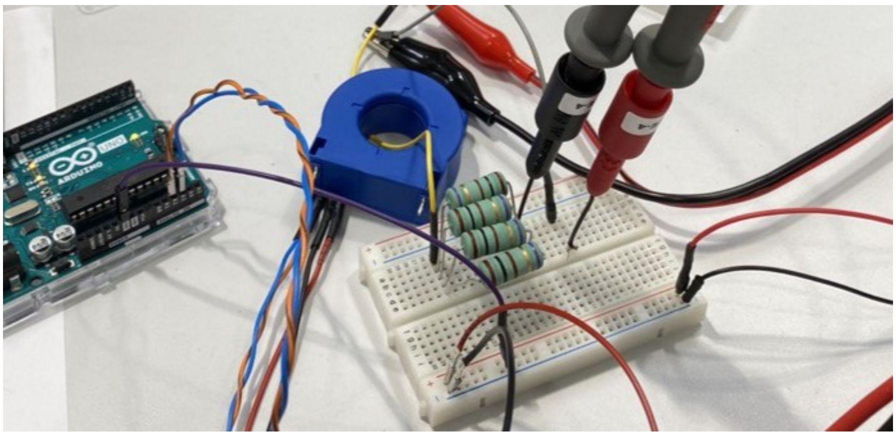

**Figure 4.16:** Bredboard testing: HALL SENSOR individual

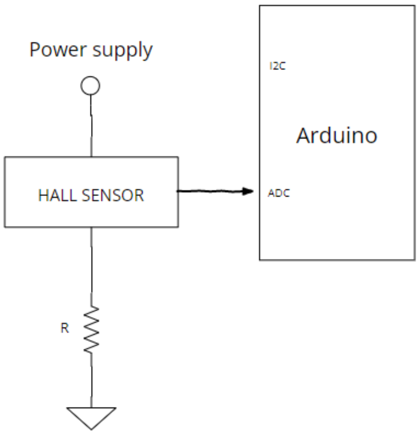


**Figure 4.17:** Bredboard testing: HALL SENSOR individual electrical scheme

As discussed before, this type of sensor has a voltage-output, consequentially the Arduino ADC was used to read this type of exit. The final value is not given by a single output, but it is measured on the base of a reference voltage, therefore 2 different ADC pins have been used to obtain the final voltage.

**Hall Sensor programming:** In this case the program was simple, due to the fact that no libraries were requested. The program just had to read both ADC values coming from the voltage-outputs of the Hall sensor and successively to compute the difference between the output and the reference voltage.

```
int analogPin2 = 2;
int analogPin3 = 3;
int vref = 0;       // variable to store the value read
int vout = 0;
void setup()
{
  Serial.begin(9600);                // serial speed setup
}
void loop()
{
  float sommavref=0;
  float sommavout=0;
  int i;
  float voltagevref=0;
  float voltagevout=0;
  for(i=0;i<100;i++){
  vref = analogRead(analogPin2);    // vref su pin 2
  vout = analogRead(analogPin3);    // vout su pin 3
```

```
  voltagevref = vref * (5.148 / 1023.0);
  voltagevout = vout * (5.148 / 1023.0);

  sommavref=voltagevref+sommavref;
  sommavout=voltagevout+sommavout;
 }
  Serial.print("Vout=");
  Serial.println(sommavout/100-sommavref/100,3);
  Serial.print("Current=");
  Serial.println((sommavout/100-sommavref/100)/1.2,3);
  Serial.print(millis());
}
```

To filter the noise in the measurement, it has been added a small software averaging over a certain number of sampling. The main problem is given by the fact that since it is not present an internal function that does it automatically, such in the INA226, it steals time from the Arduino loop, slowing down the execution speed and consequentially decreasing the sampling rate. In the case of multichannel device, each measurement requires a large amount of time, overcoming the predefined requirement.

Thanks to the similar behavior and structure, the LESR 6-NP has been tested in the same configuration of the CTSR 1-P. The results have been compared with the measurement collected by the multi-tester, they were comparable overcoming the threshold of 300 mA (table 4.2).

Since the component worked properly also in the low current range, the LESR 6-NP has been chosen to be implemented in the prototype. This has been done in order to cover the entire high current range using only one hall sensor.

**Switching logic:** In the chosen design, the choice of this component is a very critical task. This element required a very high reliability, since the protection of the shunt resistor in the high current range is dependent on it. Firstly, to do this it was taken in consideration a normal switch but since the instrument has to be auto-ranged, there was not a further research in this direction. Secondly it has been taken in consideration a relay, but it was an obsolete solution since the switching speed did not satisfy the system needs.
Subsequently, it has been taken in consideration to use a N-Mosfet parallel with the shunt resistor, but it has been put aside for two different reasons: first, the high side transistor driving is not a straightforward task because it requests specific high side driver circuit, such as the charge pump; second, the choice of the N-MOS is not trivial due to the fact the $R_{ds,on}$ of the Mosfet could be comparable with the

| **Multi-tester Current [mA]** | **LESR 6-NP current [mA]** | **Measurement error %** |
|---|---|---|
| 50 | 30 | 40,0 |
| 100 | 87 | 13,0 |
| 200 | 186 | 7,0 |
| 300 | 290 | 3,3 |
| 400 | 385 | 3,8 |
| 500 | 494 | 1,2 |
| 600 | 597 | 0,5 |
| 700 | 698 | 0,3 |
| 800 | 800 | 0,0 |
| 900 | 903 | 0,3 |
| 1000 | 1006 | 0,6 |
| 1100 | 1106 | 0,5 |
| 1200 | 1209 | 1,0 |
| 1300 | 1313 | 1,0 |
| 1400 | 1413 | 0,9 |
| 1500 | 1511 | 0,7 |

**Table 4.2:** Current results LESR 6-NP

Shunt resistor value.
Finally, it has been chosen a proper SSR element, the Sensata CMX60D20. This component does not need a specific driving control circuit, but it can be driven directly by the Arduino digital output (5 V digital exit); it has a fast response time between the switching from ON to OFF and vice-versa; it has a quite reliable behaviour, with a ultra low $R_{ds,on}$ not comparable with the Shunt resistor value and finally it can support considerably high currents and quite high input voltages on the HV side. (All the specifications are reported in the tab: 4.3).

In the figure (4.18) it is shown a picture of the component: as it can be seen on the left side is located the control circuit (LV) instead on the right side is located the MOSFET output (HV).
Anyway in this kind of circuit with shunt resistor, it has to be taken in consideration the power dissipation. Besides the idea of short-circuiting the shunt resistor in the high current range. To avoid the burn-out of the resistance in the case of failure (or in the transient time). It has to be ensured that for high current the shunt resistor can dissipate all the requested power or in any case it must be protected. This task can be done by paralleling the shunt resistor with a Zener diode, that ensure a fixed voltage across it, also in case of malfunction.


**Figure 4.18:** Sensata CMX60D20

| Specifications | Value |
|---|---|
| Control Voltage | 3-10 V |
| Operating voltage | 0-60 V |
| Maximum load current | 20 A |
| Minimum ON-state resistance | 0,0033 Ω |
| Maximum ON-state voltage drop at rated current | 0,1 V |
| Maximum turn-On Voltage | 3 V |
| Minimum turn-Off voltage | 1 V |
| Input current | 15 mA at 5V |
| Maximum turn-ON time | 1 ms |
| Minimum turn-OFF time | 300 µs |
| Dimensions | 43,1x7,6x(25,4+7,6) mm |

**Table 4.3:** CMX60D20 specifications

**Switching logic programming:** Also in this case the program required to drive the the SSR was uncomplicated, to change the state between High impedance and low $R_{ds,on}$, it needs only to receive the 5 V digital output coming from Arduino digital signal.

```
int SWITCH_PIN=13;
void setup() {
  pinMode(SWITCH_PIN, OUTPUT);
}
void loop() {
  digitalWrite(SWITCH_PIN, HIGH);  // turn ON the output pin
  delay(3000);                     // wait for 3 seconds
  digitalWrite(SWITCH_PIN,LOW);    // turn OFF the output pin
```

```
  delay(3000);
}
```

In this program, the SSR switches ON and OFF continuously every 3 seconds. By using a multi-tester it has been checked the change of the impedance value that had to vary between the two different states, it worked correctly.

### 4.5.3 Breadboard testing

Subsequently the trial of each individual component and before to test the "final" breadboard circuit, it was necessary to merge all the programs together. To do this, it has been developed a block diagram, which helped during the writing of the final program. In the figure 4.19 it is shown the block diagram.

The diagram is structured as follow.
The *first step* is shorting the shunt resistor by activating the Arduino digital pin. This is done considering that at the power-up of the measurement unit, the magnitude of the current flowing is unknown.
The *second step* is the reading of the current through the Hall sensor, so that the program can understand in which range is located, the switching range has been chosen to create a sort of overlapping between the hall sensor and the shunt resistor measurement.
The *third step* is the choice of the proper sensor depending on two different thresholds, at this point the program has to choose between two different branches. On the right, as long as the read current remains over a certain threshold, it continues reading the output coming from the hall sensor through the ADC. At the same time, it keeps high the Arduino digital exit in order to maintain the short circuiting across the shunt resistor. On the left, it enters in a different loop where it continues reading the output of the INA226 (through the I2C), and simultaneously it continues checking the hall sensor current value. This operation is done until the current value remains below a second threshold. In the same time the Arduino digital exit is LOW and consequently the switch is open.

A key feature is to create a sort of hysteresis having 2 different current thresholds, one for the Hall sensor range and the second one for the shunt resistor range. This is necessary, in order to avoid a fast commutation between the two sensors. This problem could happen in the case of a single threshold.
The two thresholds have been computed considering two different parameters: the minimum current detectable by the hall sensor and the maximum current that can flow inside the shunt resistor. As mentioned above in the table 4.2, the Hall sensor can detect current larger than 300 mA. Consequently, the first threshold

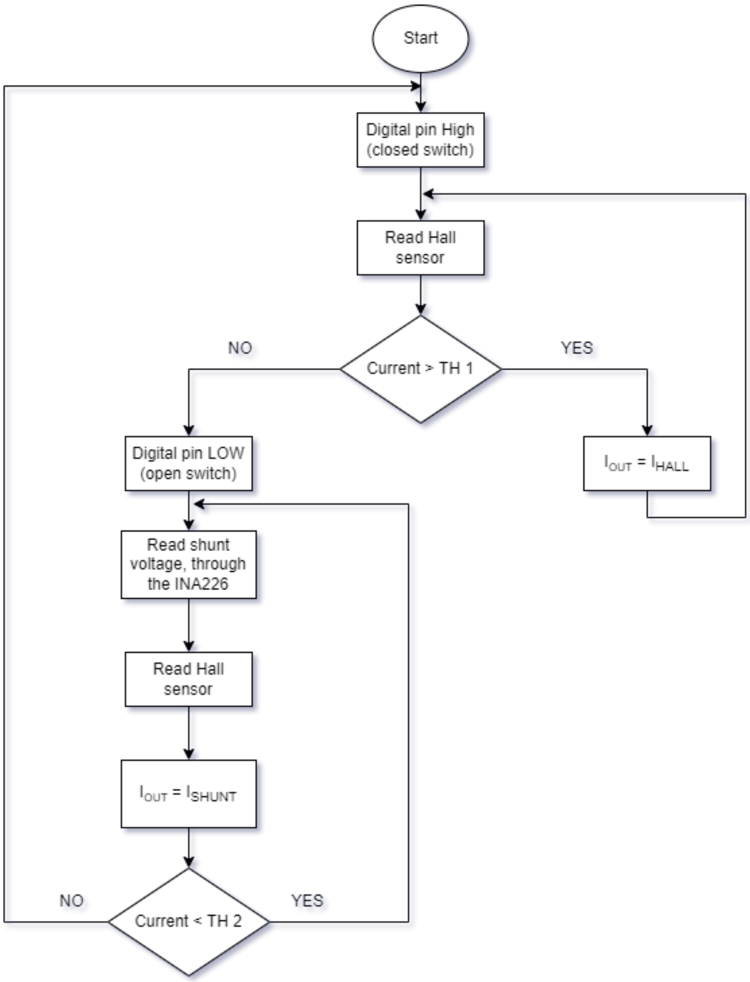


**Figure 4.19:** Block diagram prototype

(TH1) was fixed at 400 mA. The second threshold (TH2) depends on the maximum current that can flow in the shunt resistor ($\approx 800\,\text{mA}$). This value has been fixed at 500 mA to be conservative.
In the following will be highlighted the main part of the program, the initialization phase is not shown since it is present aforementioned where the individual parts of the program are described.

```
 void setup()
 {
  pinMode(SWITCH_PIN, OUTPUT);
  digitalWrite(SWITCH_PIN,HIGH);
void loop()
{
```

```
int j=0;
static char sprintfBuffer[100];
static char V_LESR[15], I_LESR[15],V_SHUNT[15], I_SHUNT[15];
media_fn();                                     // average function
Vlesr=(sommavout-sommavref)/media;
Ilesr=Vlesr/0.1042;                              //Hall sensor current
Ishunt=ina.readCurrent() * 1000;                 //Value in mA
Vshunt=ina.readShuntVoltage();                   //value in mV
sommavout=0;
sommavref=0;
if (Ilesr > 0.4)
{
  dtostrf(Vlesr      , 9, 3, V_LESR);
  dtostrf(Ilesr      , 9, 3, I_LESR);
  dtostrf(Vshunt     , 9, 3, V_SHUNT);
  dtostrf(Ishunt     , 9, 3, I_SHUNT);
  sprintf(
    sprintfBuffer,
    "HALL:  V_LESR = %s V I_LESR = %s A V_SHUNT = %s mV I_SHUNT = %s mA\n",
    V_LESR, I_LESR, V_SHUNT, I_SHUNT
  );
  Serial.print(sprintfBuffer);
  Serial.print(millis());
}
else
{
  digitalWrite(SWITCH_PIN,LOW);      //Finish short circuiting
  do
  {
    j=j+1;
    voltagevref = analogRead(analogPin2) * (5.148 / 1023.0);
    voltagevout = analogRead(analogPin3) * (5.148 / 1023.0);
    sommavref  = voltagevref + sommavref;
    sommavout  = voltagevout + sommavout;
    if (j==media)
    {
      Vlesr = ( sommavout - sommavref )/media;
      Ilesr = Vlesr/0.1042;
      sommavout  =0;
      sommavref = 0;
      j=0;
    }
    Ishunt=ina.readCurrent() * 1000;             //Value in mA
    Vshunt=ina.readShuntVoltage();               //Value in mV
    dtostrf(Vlesr  , 9, 3, V_LESR);
```

```
      dtostrf(Ilesr  , 9, 3, I_LESR);
      dtostrf(Vshunt , 9, 3, V_SHUNT);
      dtostrf(Ishunt , 9, 3, I_SHUNT);
      sprintf(
        sprintfBuffer,
        "INA226:   V_LESR = %s V I_LESR = %s A V_SHUNT = %s mV I_SHUNT = %s mA\n",
        V_LESR, I_LESR, V_SHUNT, I_SHUNT
      );
      Serial.print(sprintfBuffer);
      Serial.print(millis());
    }  while (!(Ilesr > 0.5 || Ishunt > 500) );
    digitalWrite(SWITCH_PIN,HIGH);      //SHORTING THE SHUNT RESISTOR
  }
}
```

In the program, it is possible to distinguish 3 main blocks: SSR Driving, INA226 reading and Hall sensor reading. To check and monitor the behaviour of the algorithm, all the measurements were printed on the Arduino Serial Monitor. In this first version of the program, besides the value of the current, the INA226 was able to read the Bus voltage (this feature was removed later). The measures coming from both sensors were followed by millis value, necessary to estimate the loop time. As last, it was also present the software averaging function, required to remove noise from the Hall sensor output.
After the programming phase, it has been proceeded with the mounting of the 3 different components on a single breadboard.

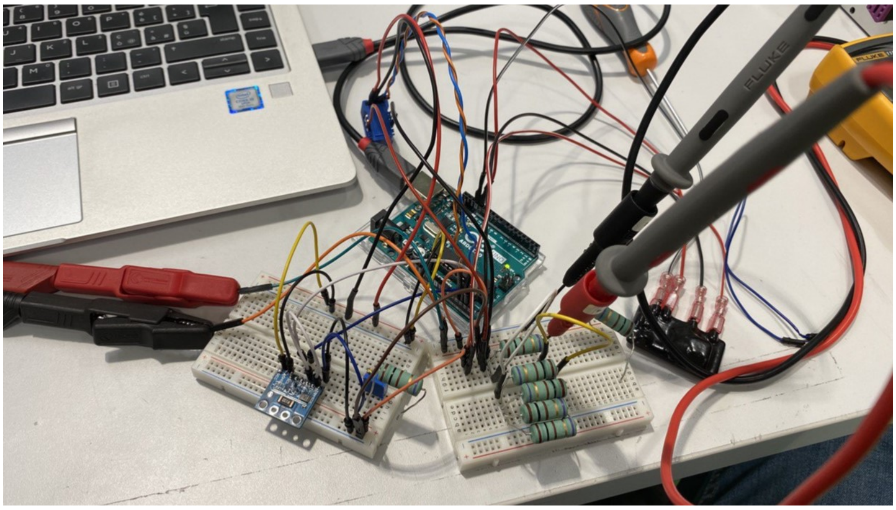

**Figure 4.20:** Bredboard testing: Sensor fusion

This configuration was mainly used to understand if the idea developed during the concept phase was feasible. It has been checked especially the operating on the threshold values, trying to see if using the chosen thresholds the fast commutation was avoided.
The setup worked correctly, but due to the high number of limits given by the breadboard, such as: the not negligible internal breadboard tracks resistance or the current limits of the connectors, it was not deepened the behaviour of this breadboard configuration. But it was taken care especially to the operating on the thresholds. Anyway with this configuration it was measured up to 500 uA and an upper limit of 1 A (compared with the oscilloscope).
This upper current limit was not overcame, due to the fact that in the company it was not present a resistor able to dissipate high power value. After these last trials, the next step was the concept and the design of the first prototype of the instrument.

## 4.6 Prototype

Since the configuration developed on the bredboard worked correctly, before to proceed with the final PCB circuit, it has to be done further tests and considerations. Thanks to the fact that in the company is present a milling machine, the first prototype was a milled circuit, where several breadboard limitations could be overcome (i.e. tracks resistance or current limits).
In order to create the necessary files required to produce the circuit, it was used KiCad, it is an open source suite of software Electronic Design Automation for the technical drawing of electrical circuit and printed circuit (PCB).
Also in this case, several steps are followed to reach the design of the circuit board.

**Sizing:** The working area in this milled test circuit had not yet been taken in consideration, this is due to the fact that it was not supposed to be insert in the final testing environment, consequently it was not required to respect a predetermined size limits.
The choice of the final size was dependent by another factor. The cutting tip did not possess very high accuracy, consequently it was very important to choose the proper width for each track in order to not overlap the adjacent paths. For the same reason it was also requested an high amount of copper around each hole and connector.

**Electrical circuit:** The aim of the wiring diagram is to track all the connections between the different components. Since the design libraries of the switch (CMX60D20) and the hall sensor (LESR 6-NP) were not included in the program,

it was necessary to add both. For both components it was necessary to create from scratch, since the manufacturers do not provide the files.
Regarding the INA226, thanks to the fact that it is provided directly on a PCB module, it was only required to choose the proper connector. The same was done for Arduino UNO, it was not designed a plug-and-play space, but simply a connector with the necessary pins.
Since this configuration was mono-channel Arduino could power all the components with his 5 V exit, remaining under the limits of the Arduino voltage regulator equal to 30 mA. Besides the LV connector it was also present the HV connector. In the figure (4.21) it is shown the complete electrical circuit.

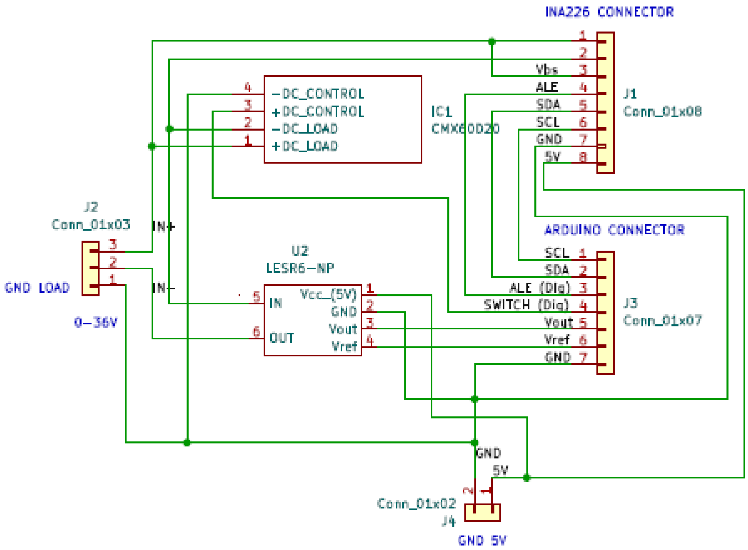


**Figure 4.21:** Prototype electrical scheme

**Wires routing:** Subsequently the electrical design, the next step was to allocate manually each component and to track the paths. In order to do this, since the circuit was milled, it was mandatory to place all the paths using only one side of the board. This operation could be done also automatically but given the reduced number of components, it has been preferred to do this operation manually. Following in figure 4.22 it is shown the final result.

**Final realization:** For creating the final circuit, the cutting machine requests the Gerber files: border file, holes file and lastly the file related to the paths. These files are generated directly by KiCad. Following it is shown a picture of the milling machine during its motion (fig 4.23).

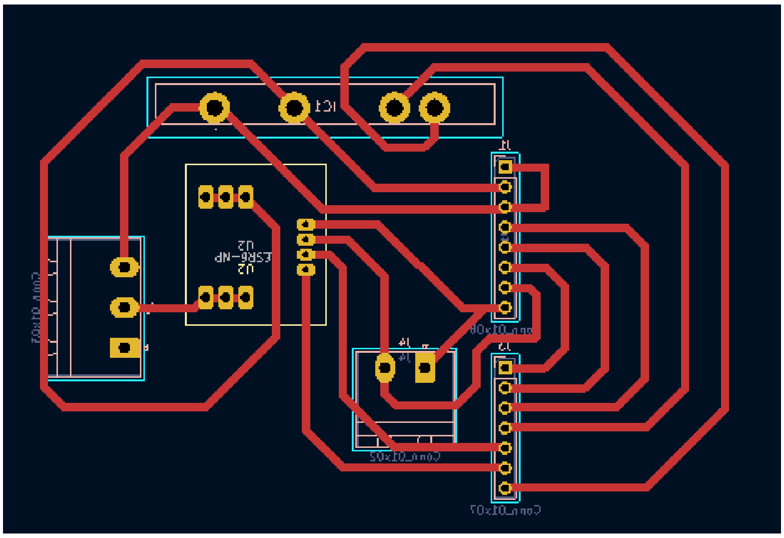

**Figure 4.22:** Prototype printed board

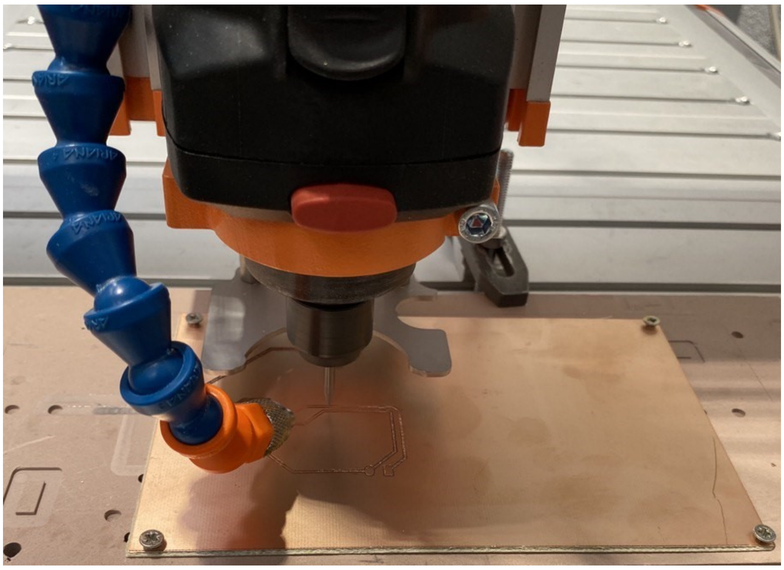

**Figure 4.23:** Milling machine operation

Finally, after soldering all the components, it is shown the final result (fig 4.24 and fig 4.25).

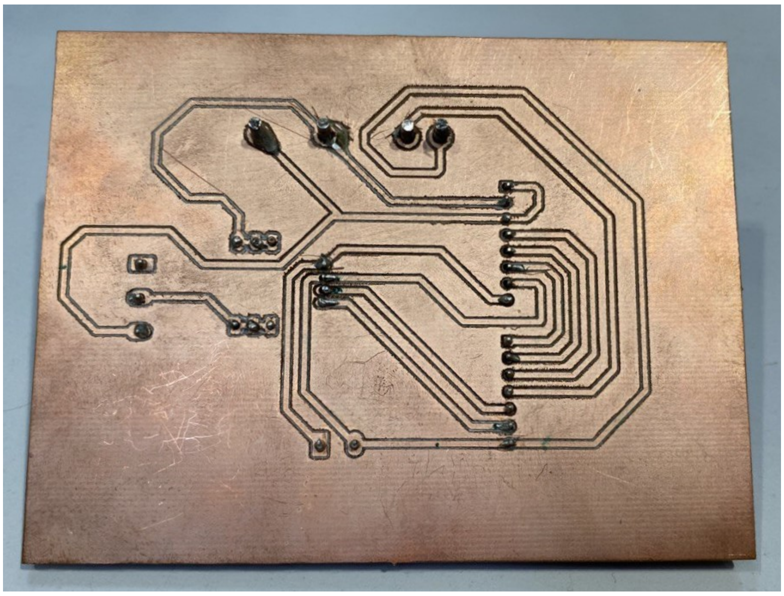

**Figure 4.24:** Final result back

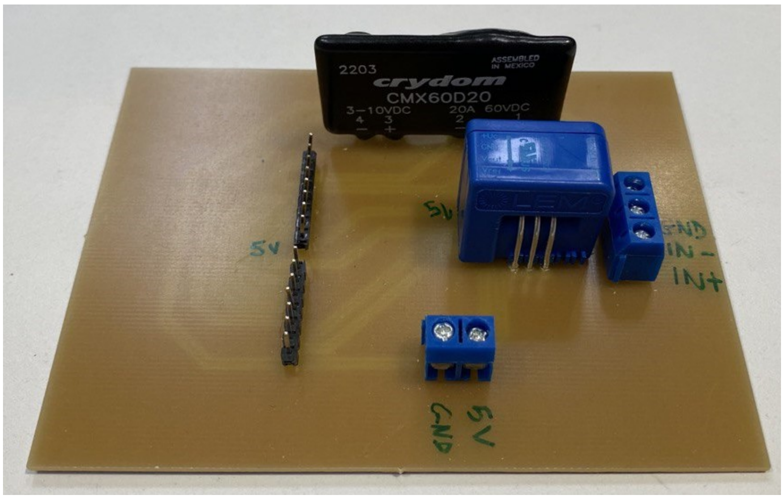


**Figure 4.25:** Final result front

**Testing:** this analysis was divided in two different parts:

- In the <u>first test</u> the circuit was simple, the configuration used was the same as in the previous phases, composed by the power supply, the prototype (located high side) and finally by a power resistor (10 Ω 86 W). The power resistance was the only improvement compared to the configuration used in the concept development phase, since it was able to dissipate a large amount of power (fig

4.26). For varying the current flowing in the circuit, it was tuned the value of the power supply voltage. This was possible, thanks to the fact that all the components could support a wide range of input voltage (up to 36 V).

**Figure 4.26:** Power resistor

- In the <u>second test</u> the prototype was located inside the real testing environment (4.27). The measurement unit was placed high side, between the power supply and the control Units. Three different states have been tested: one in the normal operation (1,5 A); one in the sleep conditions (700 mA) and the last one in in the deep sleep conditions (3 mA). Since these values of current were known, it was not necessary to compare the output of the prototype with a second measurement device, the output results of the prototype were correct.

**Improvements:** Besides some upgrades in the code, some new features have been integrated in the prototype.

1. To enhance and facilitate the end user experience, in addition to the serial monitor interface, it has been added a small 128x64 **OLED display**. This device communicates through I2C BUS. The complete integration of the tool has been done following 2 different steps: the first was the connection and the second was the coding.
   The display has only four pins (image 4.28): there are two connectors for the supply and other two connectors for the I2C, called SDA and SCL. Every component on the bus I2C is linked in parallel with the others.

   There are several libraries on the web that can help with the specific display chip (SSD1306). After several test, Adafruit libraries [22] was the one that can fit most the requirements. The main functions of the program are shown in the following, the configuration of the initial parameters is not shown (such the address setting or the I2C setting).

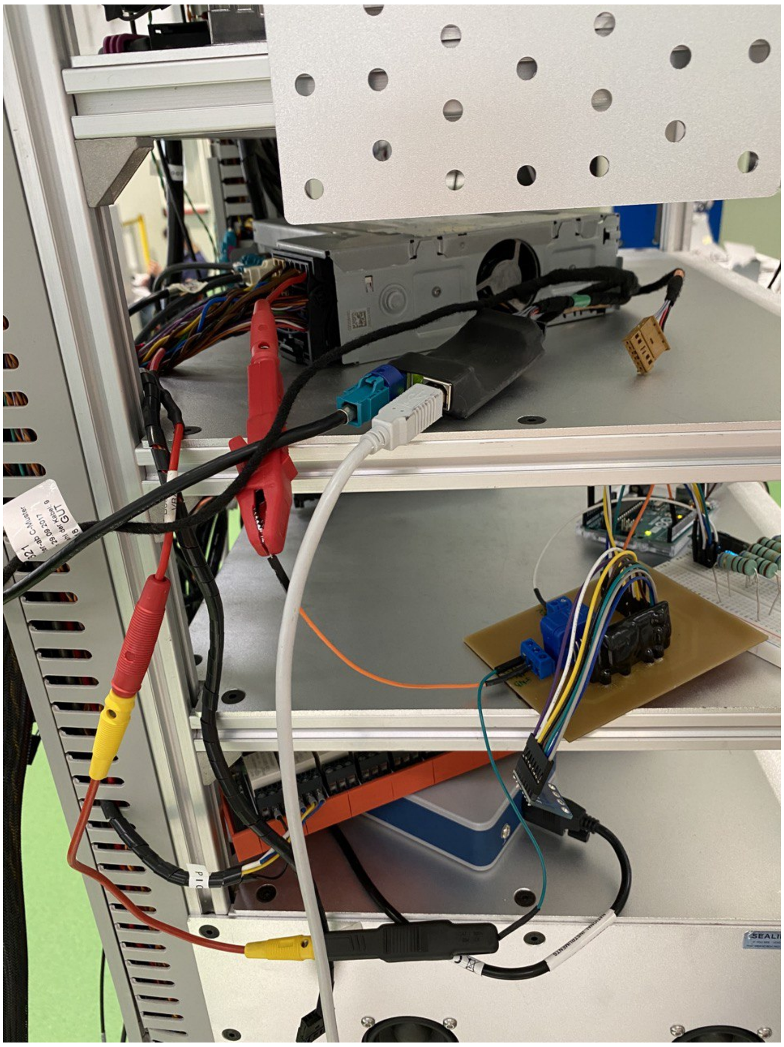

**Figure 4.27:** Trial of the prototype in the testing environment

```
display.clearDisplay();        //Clear the display buffer
display.setTextSize(1);        //Set the height
display.setTextColor(WHITE); //Set the color
display.setCursor(0,0);        //Set the cursor position
display.println("");           //Show the text on the display
```

2. As second improvement, it has been added the **CAN communication**, this needs to make available the measurements via software, for further processing. The aim of this feature is to process and memorize the measures for testing purpose. Another key feature implementable only via software, will be the synchronization between the testing environment and the current sensing

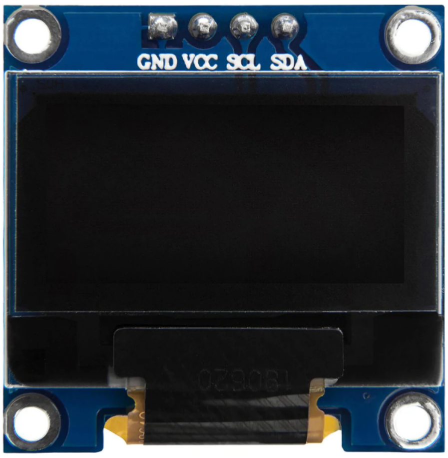


**Figure 4.28:** Display picture

device. This will be done, making accessible the exact moment at which the measure is acquired, using the millis function.


**Figure 4.29:** MIKROE CAN spi interface module

The component chosen to accomplish this task is a board made by the MIKROE company. It is a module (4.29) already equipped with all the components (such the capacitors, oscillator and the resistors) that needs for the normal operation. The main chips are the CAN transceiver MCP2561 and the CAN controller MCP2515, the first chip acts as a interface between the CAN bus and the CAN controller. As last, it is important to highlight that the communication

between the Arduino and the module is done through the SPI Interface, in order to not use too many devices one the I2C.
Also in this case the operation was divided in the wiring phase and the coding phase. The coding was done using the manufacturer libraries. The main function used to send data on the CAN BUS is shown in the following.

```
CAN.sendMsgBuf(CANaddress, 0, 8, CAN_Payload);
```

The function requests four different parameters: the ID that needs to individuate the message; the second parameter indicates if the frame is extended or not; the third needs to indicate the DLC and the last parameter is the value to be sent.

After several test and analysis, it was possible to realize and to comprehend what were the next steps to do to improve the prototype concept. The subsequent step was to realize the final design.

## 4.7 Product design

The final design took inspiration from the prototype model, it keeps the idea and the concept but some changes occurred. Since the current measurements taken in the low currents range were considerate adequate, there was not changes on the shunt resistor sensing. The speech was different for the switching logic and for the Hall transducer, even if the same design was maintained, some changes needed to be made. Lastly, since the final device should be able to measure the current simultaneously on four different channels, also the program received some adjustments.

### 4.7.1 Prototype updates

**Shunt monitor device:** As mentioned before, the current monitor device remained unchanged with the same PCB module used for the prototype. The main advantage of this configuration is the easy replacement, if there will be some malfunctions, replacing the module will be an easy, cheap and quick task. In addition, the shunt resistor is located in close proximity of the INA226 pins, consequently the noise is reduced to a minimum. The shunt resistor will be replace with the proper value to sense the sleep currents.

**Hall sensor:** This is one of the main changes compared to the prototype. The sensor produced by the LEM company had some downsides: such a significant footprint and an high cost. In the case of multi-channel capability, both peculiarities are not negligible, using four different LESR 6-NP the working area increases significantly, and proportionally the size of the printed board. At the same time also the costs become very important.
After careful researches, a worthy replacement has been found, a component made by the TI company, the TMCS1100A4. The component characteristics are shown in the table (4.4).
This device was implemented in the same way of the previous component, with the big advantage that the footprint is greatly reduced. The sensitivity is approximately the same of the previous sensor, some comparisons have been made and the results were almost the same (table 4.5). In addition, this component is able to sense current up to 12 A so it could fit perfectly the range of the testing environment. Since the component was provided one the SOIC package, in the experimental test, the transducer was soldered on a SOIC to DIP adapter. This component will be used between 300 mA up to 10 A, some software calibrations should be done to obtain a suitable measure.

| **Specifications** | **Value** |
|---|---|
| Operating voltage | 0-600 V |
| Sensitivity | 400 mV/A |
| Sensitivity error (T = 25°C) | ±0.2% |
| Supply voltage | 4,5 ÷ 6 V |
| Bidirectional capability | Yes |
| Signal bandwidth | 80 kHz |
| Maximum current | 12 A (monodirectional) |
| Output voltage offset error | ± 2.2 mV |
| Current Offset error | ± 5.5mA |
| Conductor resistance | 1.8 mΩ |
| Slew rate | 1.5 V/µs |

**Table 4.4:** TMCS1100A4 specifications

| **Multi-tester Current [mA]** | **LESR 6-NP current [mA]** | **TMCS1100A4 current [mA]** |
|---|---|---|
| 50 | 30 | 80 |
| 100 | 87 | 125 |
| 200 | 186 | 219 |
| 300 | 290 | 317 |
| 400 | 385 | 410 |
| 500 | 494 | 458 |
| 600 | 597 | 601 |
| 700 | 698 | 697 |
| 800 | 800 | 793 |
| 900 | 903 | 888 |
| 1000 | 1006 | 983 |
| 1100 | 1106 | 1078 |
| 1200 | 1209 | 1174 |
| 1300 | 1313 | 1269 |
| 1400 | 1413 | 1366 |
| 1500 | 1511 | 1464 |

**Table 4.5:** LESR 6-NP vs TMCS1100A4

After several tests, focusing on the multi channel capability, using the integrated Arduino internal ADC the requirements on the sampling time were not respected. In the table 4.6 are shown the Arduino ADC specifications.
The ADC is connected to an 8-channel analog multiplexer which allows eight single-ended voltage inputs. Using all the channels, the sampling time is decreased

| Specification | Value |
|---|---|
| Absolute accuracy | ±2 LSB |
| Integral non-linearity | 0.5 LSB |
| Sampling rate | 15 KSPS |
| channel | 8 |
| bit | 10 |
| Input voltage range | 0 to $V_{CC}$ |

**Table 4.6:** Arduino ADC specifications

by 8 times. However, the main problems related to the Arduino ADC is the fact that does not have an internal automatic oversampling function, such the INA226. Since this feature is not present, the oversampling procedure has to be done via software, employing a large amount of computational power and a large amount of time. Using the software averaging function on a single channel, the corresponding loop time was high, approximately it took 33 ms for a single measure.

To solve this problem, it has been decided to use an external multichannel 16 bit ADC, the ADS1115 (Texas Instrument). Also in this case it was necessary buying the PCB module (4.30), due to the component shortage given by the pandemic, as for the INA226.

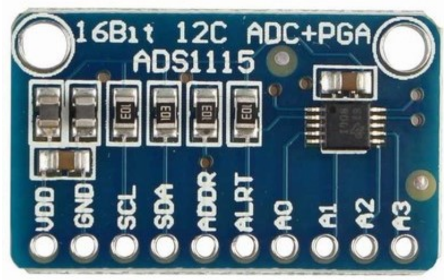


**Figure 4.30:** ADS1115 module

This device is delta-sigma ADC, with 4 different channels and communicates with external environment via I2C bus, but the biggest peculiarity is the fact that it is completely programmable. It is possible to set the voltage input range, the output data range and also to configure the oversampling operation. This last peculiarity is very important, since it avoids using the software averaging function that slowed down the main program. Lastly, it has a programmable low drift internal voltage reference. The main specification are shown in the table (4.7).

| Specification | Value |
|---|---|
| Supply range | 2.0 V to 5.5 V |
| Integral non-linearity | 1 LSB |
| Programmable Data Rate | 8 SPS to 860 SPS |
| channel | 4 |
| bit | 16 |
| Input voltage range | ±0.256 V to ±6.144 V |

**Table 4.7:** ADS1115 specifications

**Switching logic:** This is the second major change inside the final configuration. In the prototype, the switching logic was completely managed by the CMX60D20, this component was very expensive and bulky. In the case of multichannel capability, these features has to be taken into account and consequently it has been decided to replace it.
Internally (figure 4.31) the SSR is constituted by three main devices. The MOSFET that acts as a switch. The photo-diode, which is a light-sensitive device able to produce current by absorbing photons. Lastly the control circuit, which needs to discharge rapidly the photo-diode when it is not powered.

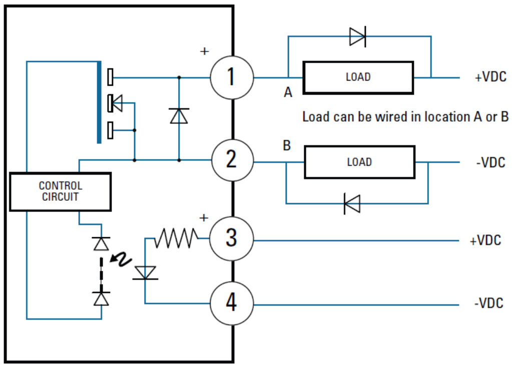


**Figure 4.31:** Wiring diagram CMX60D20

After having examined the internal circuit of the CMX60D20, it has been concluded that it was possible to reproduce the same configuration using different components. Specifically, the switching logic was composed by a specific N-MOS and by a photocoupler controlled directly by Arduino.

- The **N-MOS** has to respect some requirements: the most important is the low $R_{ds,on}$ since it must be not comparable with the shunt value; the second is the Gate-to-source threshold Voltage, which needs to switch-ON the MOS; the maximum continuous Drain current $I_D$, it has to dissipate current up to 10 A; as last but not least the maximum Drain-to-source voltage, it must support up to 30 V. The final choice was the IRLU8743 (Specification in table 4.8).

| **Specification** | **Value** |
|---|---|
| $V_{DS}$ | 30 V |
| $V_{GS}$ threshold | 2.35 V |
| $I_D$ with $V_{GS} = 10$ V | 160 A |
| $R_{DS,ON}$ | 2.4 - 3,1 m$\Omega$ with $V_{GS} = 10$ V |
| | 3.0 - 3,9 m$\Omega$ with $V_{GS} = 4{,}5$ V |
| Turn-On delay time | 19 ns |
| Turn-Off delay time | 21 ns |

**Table 4.8:** IRLU8743 specifications

In the chosen device, the parameters meet the requirements. The $V_{GS}$ is compatible with the gate driver output of 7 V. The maximum $R_{DS,ON}$ is equal to 3,9 m$\Omega$, as a consequence, with a current equal to 10 A the induced voltage across the MOS corresponds to 39 mV, this voltage does not damage the system. The $V_{DS}$ is suitable for the high side measurement. The turn-ON and turn-OFF time will be take in consideration in the next paragraph.

- The **Photocoupler** instead was a difficult choice. Due to the shortage given by the Covid pandemic, the majority of this specific component was not available. There exist different types of photo-coupler, someone is equipped with the discharging resistor (or with the control circuit) and others are provided without this peculiarity. After several analysis, it has been found the TLP591B, from the Toshiba company. It satisfied all the requirements: the output voltage and secondly the low forward current. The main specifications are shown in the table 4.9.
  As it can be seen in the table 4.8, the minimum MOSFET $V_{GS}$ is equal to 2.35 V, the output voltage provided by the gate driver is sufficient to turn ON the MOSFET.
  The forward current needs to feed the internal diode of the photocoupler, this current is imposed by the resistor in series with the 5 V Arduino digital output. This resistor is calculated by applying the Ohm's law, hence considering the forward current equal to 20 mA, the proper resistor value corresponds to 250 $\Omega$.

| Specification | Value |
|---|---|
| Forward current | 25 mA |
| Open voltage | 7 V |
| Short current | 40 µA |
| Turn On time | 0,2 ms |
| Turn Off time | 3 ms |
| Internal discharging resistor | Yes |

**Table 4.9:** TLP591 specifications

**Analysis of the LTspice simulation**: In order to understand the dynamical behavior of the switching logic it was used a Pulse voltage generator, which needs to simulate the Arduino 5 V digital output. Since the N-MOS chosen is not present on the LTspice environment, it has been used a component with the same characteristics. In this photocoupler the forward current is slightly different, consequently the corresponding resistor is higher. For the simulation of the testing environment, it has been used a voltage generator that acts as a battery and a current generator that acts as a fixed load.

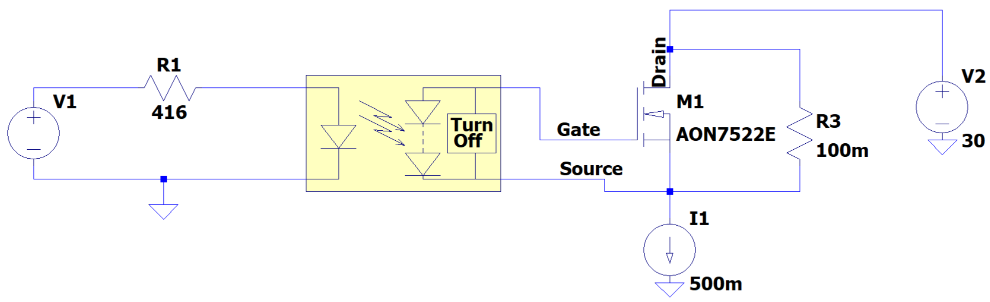


**Figure 4.32:** Switching logic LTspice electrical circuit

As it can be seen in figure 4.33 the results were adequate, the output voltage of the photocoupler follows perfectly the characteristic of the pulse voltage generator, this output is used to power the MOS and consequently to switching it ON and OFF. Lastly, the current on R3 is negligible when the MOS is turned ON and vice-versa. The switching time depends on 3 components: by the characteristics of the MOSFET and the Gate driver, and finally on the loop time of the Arduino algorithm. Taking into account the MOS specifications in the table 4.8, the turn On and turn Off time are respectively 19 ns and 21 ns. Instead the value of the photocoupler (table 4.9) are higher, respectively 0.2 ms and 3 ms. Hence, the bottleneck between

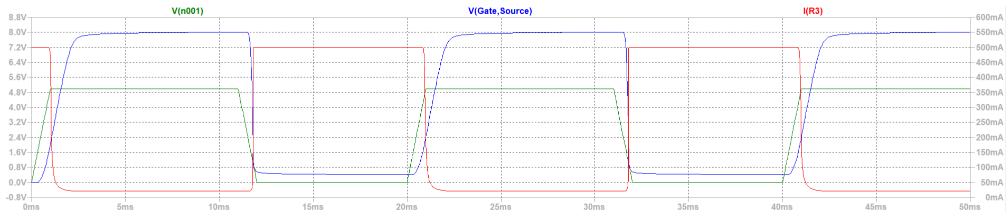


**Figure 4.33:** Switching logic LTspice characteristic

the characteristics of the two devices is the gate driver.

However, considering also the loop time of the algorithm, the current control takes place every 11 ms. As a consequence, since the Turn ON/OFF time of the photocoupler and of the MOSFET have a smaller order of magnitude, the true switching time bottleneck is the speed of the loop time. Anyway also in the case of a sharp increment of current, the automotive systems are very robust and can withstand these transients.
Considering also the shunt resistor parameters, running a fast increment of current, up to 1 A (normal operating condition). Since the resistor value is equal to 100 mΩ, also the power dissipation (0.1 W) and the induced burden voltage (0.10 V), can be managed for a short amount of time, without damaging the instrument components and without affecting the ECUs functioning. Considering the Turn-OFF time, the only drawback is the fact that in the case of a sharp current decrement, there will be a short delay in the correct measurement, without damaging the components and without affecting the ECUs functioning.

**Communication:** This part of the design has not undergone many changes, in particular the display remained the same, with the same connections. Instead the CAN communication has changed slightly, instead of using the MIKROE PCB module, the same components were employed (CAN transceiver MCP2515 and the CAN controller MCP2561), but directly soldered on the final printed board, with the proper boundary circuit suggested by the manufacturer.

### 4.7.2 New algorithm

Due to the poor computational power, the final algorithm was slight changed. In the final version, it would be perfect to use multi-threading, but since the Arduino micro-controller (ATmega328) is not multi-core, it was not possible to use this type of process. The best solution to solve this problem was using a sort of task scheduler in the final program, where each operation corresponds a specific task.
Arduino IDE provides a task scheduler library, but it is not compatible with all

the micro-controllers, the one of Arduino UNO and MICRO is not.
On the web it has found a library made by Kai Liebich and Georg Icking-Konert [23] that can run also on the ATmega micro-controller. The library works in parallel with the millis function, it allows to define a specific cycle of task, where each task has the own execution time.
This key feature is very important because it was necessary to separate the main current sensing operation with the ones used to print on the display or to send data on CAN.
Also the main algorithm was slightly changed, with this different structure, fewer operations are needed to accomplish the main current sensing operation. Parallel to this cycle, the sensed current value are transmitted on the display and on CAN bus.

As it can be seen (figure 4.34) the structure has more efficient design. The switching logic is dependent on the hall sensor and on the switch state value. The first operation of every cycle is always read the value of current sensed by the Hall transducer, after that, on the base of the predetermined current thresholds (TH1 = 400 mA and TH2 = 500 mA, previously discussed) it will be chosen the sensor to be used. In the following the key code parts.

**Main task:** The next code part is related to the main current sensing operation, it is encapsulated into a function that needs as input parameters: the INA to be considered (multi-channel capability); the Arduino digital output pin to be considered; the external ADC channel and the results of the previous operation. The first part is related to the acquisition from the ADC, the central part is the threshold assignments and the final part is the choice of the proper sensor depending on the previous parameters.

```
currentResults currentMonitor(Ina226Driver ina, int SWITCH_PIN,
int ADCchannel, currentResults inputResults)
{
  currentResults outputResults;
  outputResults.I_hall = 0;
  outputResults.I_shunt = 0;
  int s;
  int16_t valADC = ADS.readADC(ADCchannel);
  float Vhall=valADC*ADS.toVoltage(1);      //Volt
  outputResults.timestamp=millis();
  outputResults.I_hall=1000*Vhall/SensHall; //mA

  if(inputResults.activeSensor==false)
    s=sMAX;
  else
    s=smin;
```

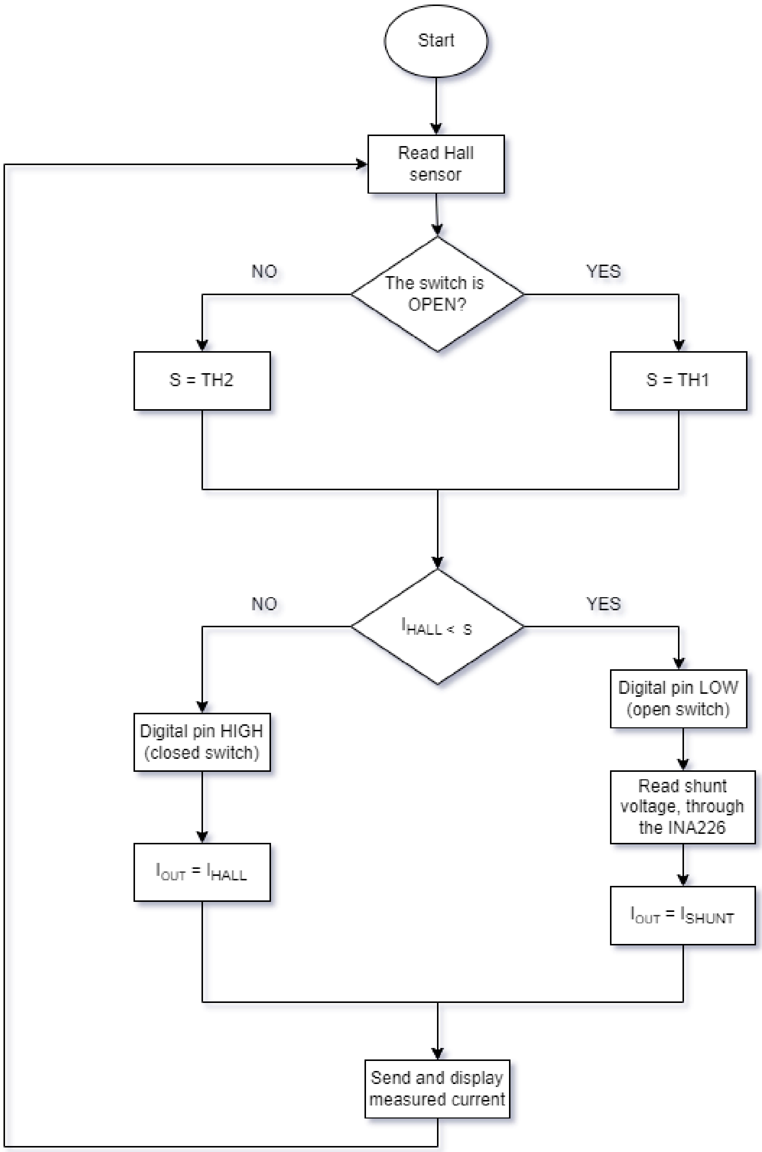


**Figure 4.34:** Block diagram final

```
if (outputResults.I_hall < s)
{
  digitalWrite(SWITCH_PIN,LOW);
  outputResults.I_shunt = ina.readCurrent() * 1000;     //mA
  outputResults.timestamp=millis();
  outputResults.activeSensor=false;
}
```

```
  else
  {
    digitalWrite(SWITCH_PIN,HIGH);
    outputResults.activeSensor=true;
  }
  return outputResults;
}
```

**Display printing:** In the following part it is shown the function needed to print the sensed measure on the OLED display. Anyway, it must be said that this operation is a kind of bottleneck for the sampling time, it needs a considerable amount of time to accomplish the printing activity ($\approx$ 200 ms). For this reason the updating of the display is set every second, less frequently than the sending on CAN.

```
void displayprint(currentResults sresults, int row)
{
    display.setCursor(0,row);
    if (sresults.activeSensor==true){
        display.print("Ihall=");
        display.print(sresults.I_hall,3);
        display.println(" mA");
    }
    else {
        display.print("Ishunt=");
        display.print(sresults.I_shunt,3);
        display.println(" mA");
    }
}
```

**CAN communication:** The next function needs to transmit data on CAN. According to the sensor used, it is chosen the proper current to send. In addition, in order to keep the timing, it is also sent the corresponding millis value of every measure. This information will be elaborated by the CAN database, for testing purpose.

```
void sendcan(currentResults eresults, const uint8_t CANaddress){
  if (eresults.activeSensor==true)
      Ican=eresults.I_hall;
  else
      Ican=eresults.I_shunt;
  CAN_Payload = (byte*)&Ican;
  CAN_Payload[4] = ((byte*)&eresults.timestamp)[0];
  CAN_Payload[5] = ((byte*)&eresults.timestamp)[1];
  CAN_Payload[6] = ((byte*)&eresults.timestamp)[2];
```

```
CAN_Payload[7] = ((byte*)&eresults.timestamp)[3];
CAN.sendMsgBuf(CANaddress, 0, 8, CAN_Payload);
}
```

**Task scheduler:** As last it is shown the part related to the task manager, in this portion is possible to set the proper timing for each operation. The function used, it is a part of the custom library, it needs as input parameters: the task to perform, how often to repeat it and the delay.

```
Tasks_Add((Task) task_main, 100, 0);
Tasks_Add((Task) task_display, 1000, 0);
Tasks_Add((Task) task_send_can, 20, 0);
```

Due to the lack of time, the final printed board has not been built yet, and as a consequence it was not possible to make a complete test of the whole operation. But anyway a single channel was tested and it worked properly. Besides this, four different INAs, the external ADC and the display have been connected to the I2C in order to test the complete operation of the new program.

**Sensor fusion:** in the solution adopted there are two different transducers, the shunt is responsible of the low current range and the hall-effect sensor is responsible of the high current range. When the switch between the two ranges occurs, it is possible to find a discontinuity in the measured current value. Since the sensors' ranges overlap in the central part, a sort of weighted average can be developed (equation 4.32), that improves the measurement's precision and avoids the discontinuity.

$$I_W = \frac{k_1 I_{HALL} + k_2 I_{SHUNT}}{k_1 + k_2} \tag{4.32}$$

Where $I_W$ is the weighted current, $k_1$ and $k_2$ are respectively the weights of the the current sensed by the hall sensor and by the shunt monitor. The weights are not constant but change linearly with the increasing and decreasing of the current. The tuning of this feature has to be done experimentally with the final product design.

### 4.7.3 Simulation

Before proceeding with the final design development, simulation campaign has been performed, to validate the concept. The SPICE libraries of the chosen components are not available on the web, consequently, MATLAB Simulink has been used to obtain significant results.
Since it was not possible to evaluate the true behavior of the components, particular attention has been paid for the switching characteristic.
The current flowing inside the ECU has been simulated by using the sum of two current generators. The piecewise generator simulates the current behaviour in different operating conditions, ranging from 1 mA up to 1 A. With this range, it is possible to evaluate the switching between the two transducers, during both the increase and decrease of the current. The noise generation has been done by using a second parallel current generator, which has been configured to reproduce a plausible noise value.
The switch parallel to the shunt needs to simulate the IRLU8743 (MOSFET) behavior and its ON resistance has been fixed equal to 3.3 mΩ, according to the datasheet.
A delay block has been inserted in the switching loop, in order to simulate the control loop with the associated loop time. Its value is fixed at 11 ms, which is the algorithm loop time. As previously discussed, the switching times of the photocoupler and the mosfet have smaller order of magnitude. In addition, a hysteresis component has been inserted, in order to avoid the fast commutation of the switch.
To simulate the INA226 acquisition, it has been used a band-limiter block. For computing the bandwidth, it has been calculated the INA sampling time $t_S$:

$$t_S = t_C \cdot n_{AVG} = 140\,\mu\text{s} \cdot 64 \approx 9\,\text{ms} \tag{4.33}$$

where $t_C$ is the conversion time, in this application is set equal to 140 $\mu$s and $n_{AVG}$ is equal to the number of measures for the averaging function. Subsequently, the frequency:

$$f = \frac{1}{t_S} = \frac{1}{9\,\text{ms}} = 111.11\,\text{Hz} \tag{4.34}$$

The corresponding bandwidth, according to the Nyquist theorem is roughly the half of the sampling frequency, hence the Bandwidth of the band limiter is set equal to 55 Hz.
The Hall sensor model is implemented by a MATLAB function block. This block is used to add the noise in the final measurement and it has been used to highlight the operating range of the sensor. For this purpose, the output of this block will provide zero if the current is lower than 400 mA. The final simulink model is shown in the fig 4.35.

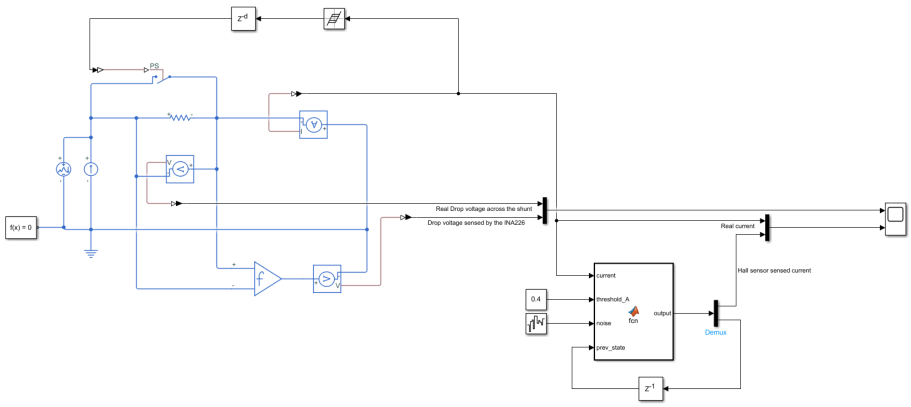


**Figure 4.35:** Simulink model

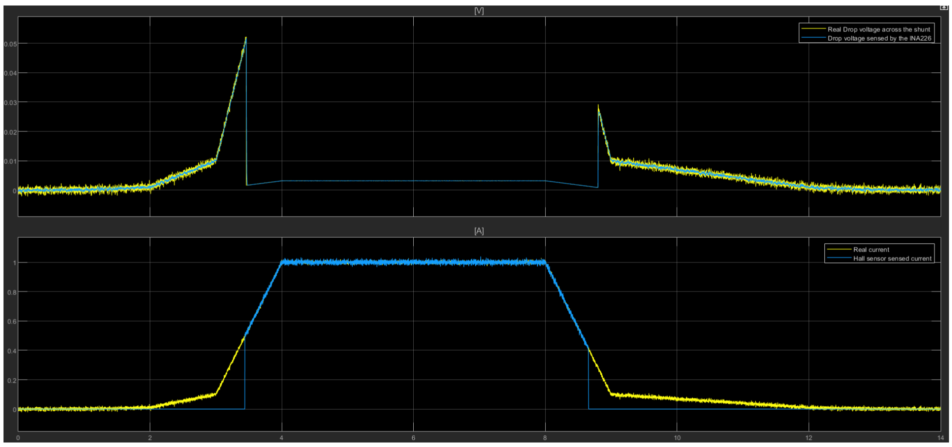


**Figure 4.36:** Output exit

The outputs of the system are represented in the fig 4.36. In the first graph two traces are shown. The yellow line represents the real voltage drop across the shunt resistor, the blue line represents the voltage drop sensed by the INA226.
An important fact to be highlighted, it is the effect caused by the loop time. The threshold is set equal to 400 mA, this means that the corresponding threshold voltage across the shunt is 40 mV.

$$V_T = R_{SHUNT} \cdot I_{TH} = 100\,\mathrm{m\Omega} \cdot 400\,\mathrm{mA} = 40\,\mathrm{mV} \tag{4.35}$$

As it can be seen in fig 4.37, due to the delay introduced by the loop time, the sensed voltage is not 40 mV but higher, roughly 50 mV. This means that the threshold voltage is properly chosen in order to stay within the INA226 ADC limit, equal to 81.92 mV.

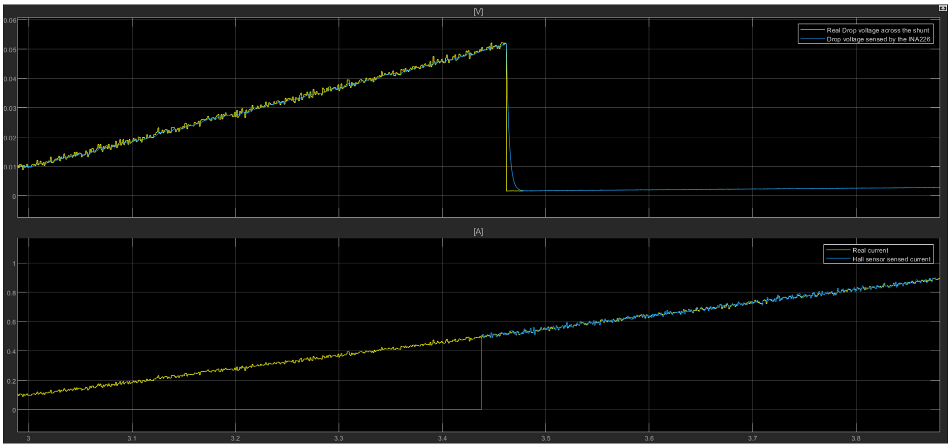


**Figure 4.37:** Delay on the switching time

Overcoming the threshold voltage, the switch has a smaller value of resistance:

$$R_{TOT} = (\frac{1}{R_{SHUNT}} + \frac{1}{R_{SWITCH}})^{-1} = (\frac{1}{100\,\mathrm{m}\Omega} + \frac{1}{3.3\,\mathrm{m}\Omega})^{-1} = 3.2\,\mathrm{m}\Omega \qquad (4.36)$$

As a consequence, flowing a current of 1 A, the sensed voltage becomes almost negligible, approximately it will be 32 mV.

In the second graph (fig 4.36), the yellow line represents the real current behavior. The blue line represents the current sensed by the hall sensor, before the threshold limit, the current coming from the Hall sensor is not considered. The simulation is not carried out above 1 A, since the behavior of the Hall current sensor would remain the same.

In conclusion this simulation represents an ideal case, which is useful to understand the final concept operating principle.

### 4.7.4 Final realization

As for the prototype, the realization of the printed board is composed by two steps, the schematic and the wires routing. As mentioned above, due to the lack of time there was not the possibility to develop the finished product, but the Gerber files containing all the necessary information for the realization of the final board are ready, these files will be provided to an external company which will have to take care of the realization of the finished board.

**Electrical scheme:** In the next page is represented the electrical scheme of the final board. As discussed before, the final device must be able to sense current coming from four different automotive control units. Thus, on the left part of the scheme is possible to observe the four different channels. Each channel is composed by the high voltage connector, the mosfet, the gate driver, the hall-effect sensor and the current shunt monitor. The output voltage coming from the hall-effect sensor is read by the external ADC placed in the central part next to the microcontroller. The Arduino UNO version has been replace with the MICRO version. This was done to shrink the overall board size, in addition the Arduino Micro is provided with the pin header connector, for a superior PCB integration.
Besides the current sensing part, on the top right part of the scheme the CAN communication can be seen. Which has been implemented with the MIKROE external module scheme, used for the prototype. To achieve better compatibility, the CAN bus is provided by both a db-9 and a phonenix connector MSTB.
Additionally, in the bottom right part, it has been implemented a LDO voltage regulator through the LM317. The 12 V line coming from the power supply is used to feed the Arduino micro. On the other hand the 5 V output of the LM317 is used to supply the transducers and the CAN communication devices.

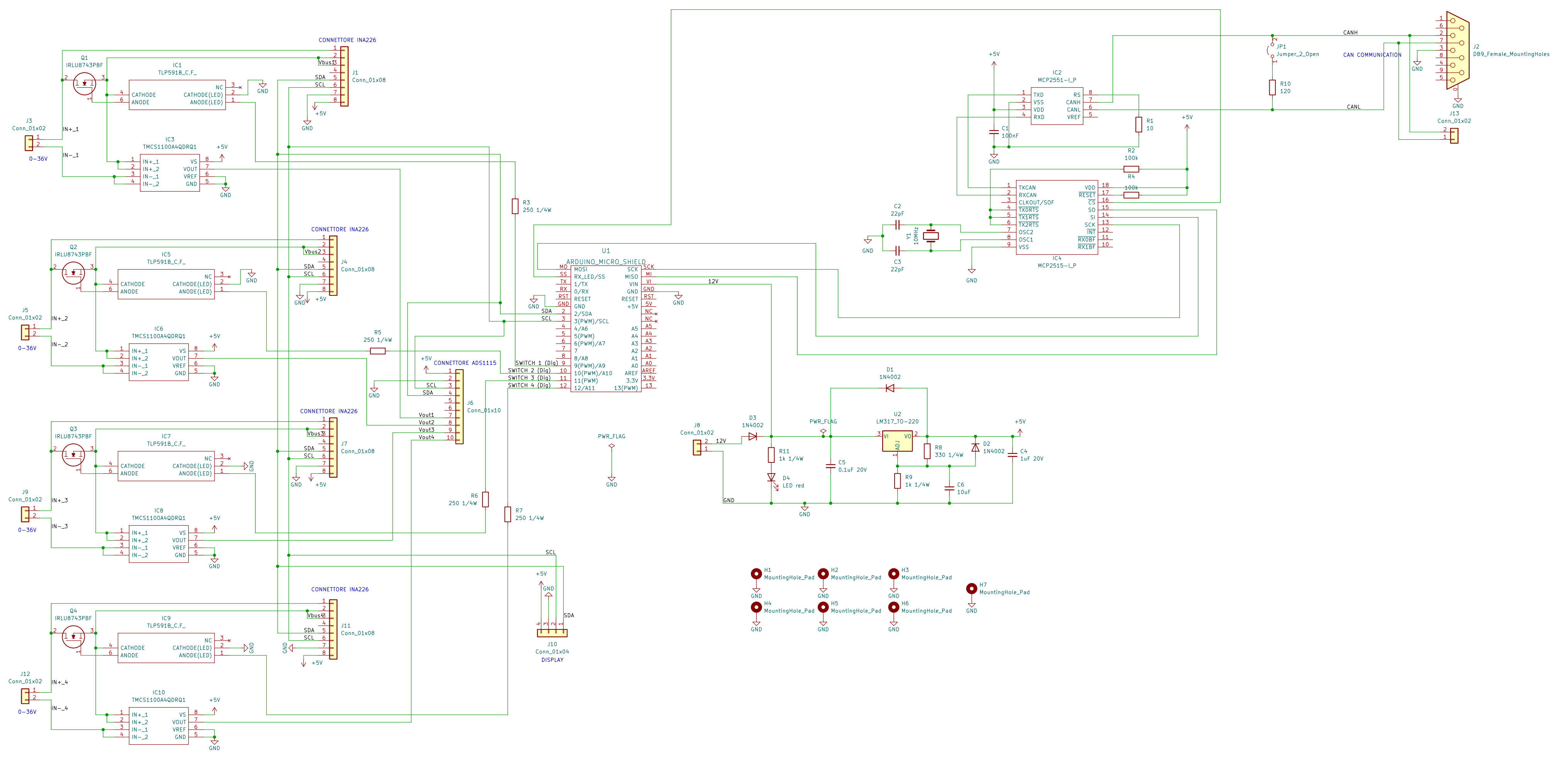


Sheet: /
File: Prova_3.kicad_sch

**Title:**

| Size: A2 | Date: | Rev: |
|---|---|---|
| KiCad E.D.A. kicad (6.0.5) | | Id: 1/1 |

**Wires routing:** In this case due to the large number of connections, it was not possible to use a single side of the board, consequently it has been chosen to use the top and the bottom of the board. The components are placed as close as possible to avoid parasitic effect. The effective size of the board is 164 mm x 108 mm. Two different widths of the trace have been used: 0.3 mm (11.81 mils) for the low power signals and for the current shunt monitor; suitable pads for the high current signals, in order to dissipate the required power.
Due to the several number of ground references, a ground plane has been introduced in the bottom part of the board. In the figure 4.38, it is represented the final layout on the board, where the blue represents the bottom copper parts and the red correspond to the upper copper parts.

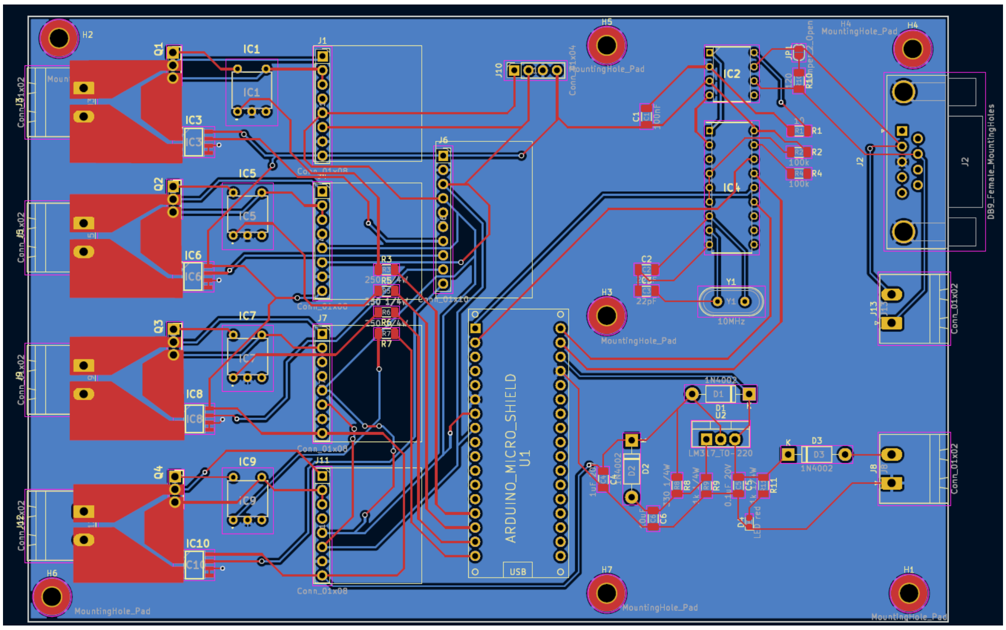

**Figure 4.38:** PCB layout

### 4.7.5 Final virtual model:

Finally the figure 4.39 represents the preview of the final printed board.

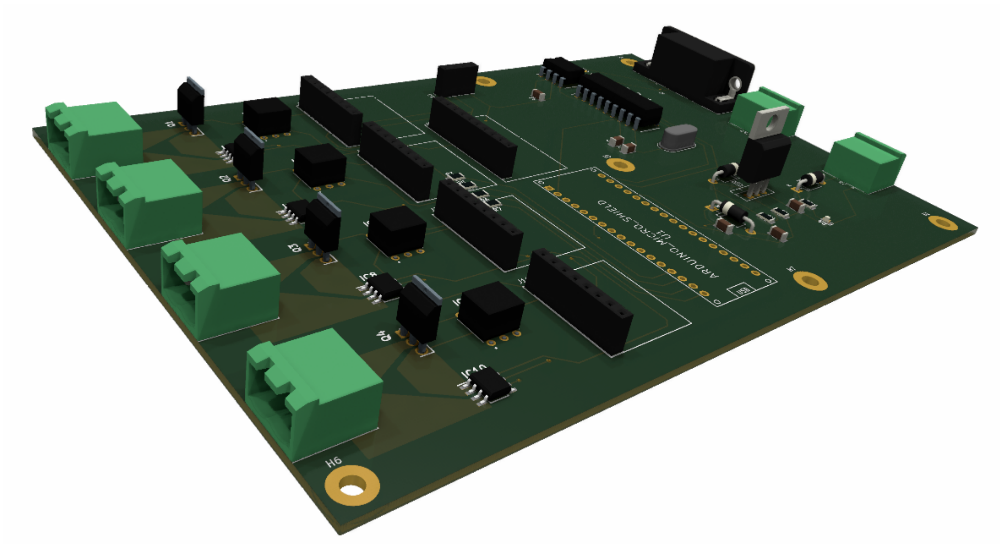

**Figure 4.39:** Board 3D preview

# Chapter 5

# Conclusion and future developments

This project aimed to study and develop a system able to monitor the current drained by different ECUs, by placing it in automotive testing environments. The idea was to achieve a device that is able to satisfy the requirements, keeping in consideration the solutions already available on the market and also taking into account the economic impact. Consequently, it has been important to reach a solution composed by easily available hardware components, which leads to a simple replacement in case of failure. Firstly, in order to define the requirements, an experimental campaign has been carried out to obtain relevant data. Based on this information, different current sensing principles have been discarded, leading to a configuration composed by two different current transducers. A shunt resistor has been chosen for the low current range and a hall sensor for the high current range. One of the main features owned by this solution, it is the auto-range capability, which allows to monitor the current drain not only in the normal operating condition but also in the system sleep mode. Both transducers have been acquired through dedicated ADCs, which communicates through i2c. After coding the algorithm on the Arduino platform, a single channel prototype device has been manufactured. This gave the possibility to understand the limits of the selected components. Another key element is the possibility to communicate through CAN bus. This peculiarity allows sending the sensed data for further processing to the test environment.
After the production and the testing of the prototype, the project has been directed towards the conception of the final board. The final system has been designed to sense the current coming from four different ECUs, resulting in the possibility to keep under control different operating devices.
It is worth to say that the device has been developed mainly on the company

need, but, thanks to the design of the system, it can be employed also for other testing equipment. One of the advantages of this configuration is indeed the possibility to replace both sensors. In case of low current sensing, replacing the shunt resistor and customizing the software would allow to increase or decrease the sensed range.Similarly, for high currents it is possible to choose a different hall sensor.

One of the main limitations of this project has been the global component shortage, which slowed down the advancement of the job, by limiting the choice on a restricted number of components. For this reason, it was not possible to obtain the final board before the end of the internship. However, the complete board design has been finalized, and simulations have been carried out in order to better evaluate the system behavior.

Consequently, the first future development will be the fabrication and the testing of the final concept board, including the sensor fusion weighted average function in the algorithm. Secondly, for decreasing the disturbances and the board size, it will be important to update the design with the components which were not available during the activity.

Successively, in order to increase the overall performance, Arduino could be replaced with a main processing unit with a larger computational power. This would give the possibility to implement a multi-threading technique, so that the main current sensing task would be speeded up, since it will not be interrupted by the other tasks. Consequently, the update of the display and the CAN communication would not interfere with the main task, thus increasing the output data frequency.

To sum up, this master thesis resulted in a meaningful approach to have an adaptive current sensing. The project validity has been proven by a single channel prototype and system simulations. Altough the critical global component shortage did not allow the realization of the final board, its design has been completed.

During further developments the device will be tested and verified in a real testing environment.

# Bibliography


[1] LinkedIn Italdesign company. URL: https://https://www.linkedin.com/company/italdesign-official/about/. (accessed: 05.09.2022) (cit. on p. 4).

[2] Wikipedia. *Electric current*. URL: https://en.wikipedia.org/wiki/Electric_current#cite_note-horowitz-1. (accessed: 05.09.2022) (cit. on p. 5).

[3] Wolfram TEPPAN Eric FAVRE. «Current Sensing in Electric Drives, A Future and History Based on Multiple Innovations». In: *LEM group* (). (accessed: 03.09.2022) (cit. on p. 6).

[4] S. Bestley Joe, T. Gomathi, D. Marshiana, and N. R. Krishnamoorthy. «Effects of Joule heating on the Temperature-Voltage Relationship in Copper». In: *IEEE* (2021). (accessed: 18.09.2022) (cit. on p. 8).

[5] Chinh T. Nguyen Ryszard Malewski. «Elimination of the Skin Effect Error in Heavy-Current Shunts». In: *IEEE* (1981). (accessed: 09.09.2022) (cit. on p. 10).

[6] ZieglerSilvio. «New current sensing solutions for low-cost high-power-desnity digitally controlled power converters». In: *University of Western Australia* (). (accessed: 03.09.2022) (cit. on pp. 10, 12, 17–19).

[7] Steve Arar. *Resistive Current Sensing: Low-Side vs. High-Side Sensing.* 2021. URL: https://www.allaboutcircuits.com/technical-articles/resistive-current-sensing-low-side-versus-high-side-sensing/. (accessed: 06.09.2022) (cit. on pp. 12, 13).

[8] Bill Giovino. *Making Sense of Current Sensing.* URL: https://www.mouser.com/pdfdocs/CurrentSenseWhitePaper-2.PDF. (accessed: 06.09.2022) (cit. on p. 12).

[9] Asha Patel and Mehdi Ferdowsi. «Current Sensing for Automotive Electronics—A Survey». In: *IEEE* (2009). (accessed: 13.09.2022) (cit. on pp. 14–16, 18, 19).

[10] Larry Spaziani. «Using Copper PCB Etch for Low Value Resistance». In: *Texas instrument* (2001). (accessed: 09.09.2022) (cit. on p. 14).

[11] *EV1025 current measuring board*. Datasheet (cit. on p. 21).

[12] *DMM7510 7½-Digit Graphical Sampling Multimeter, datasheet*. Datasheet (cit. on p. 22).

[13] *Current measurement with auto-ranging yields 180dB range dynamics*. Datasheet (cit. on p. 22).

[14] *Joulescope™ JS110 User's Guide Precision DC Energy Analyzer*. Datasheet (cit. on p. 22).

[15] *SPECIFICATIONS PXI-4065*. Datasheet (cit. on p. 23).

[16] Vector. URL: `https://www.vector.com/it/it/prodotti/products-a-z/hardware/vt-system/vt7001/#c197752`. (accessed: 08.09.2022) (cit. on p. 23).

[17] *Current Transducer LESR series datasheet*. Datasheet. 2020 (cit. on p. 43).

[18] *Current Transducer CTSR 1-P datasheet*. Datasheet. 2018 (cit. on p. 43).

[19] ArduPicLab. *The ArduINA226 power monitor*. 2020. URL: `http://ardupiclab.blogspot.com/2020/03/the-arduina226-power-monitor.html`. (accessed: 08.09.2022) (cit. on p. 46).

[20] *INA226 High-Side or Low-Side Measurement, Bi-Directional Current and Power Monitor with I2C Compatible Interface*. Datasheet. 2015 (cit. on p. 46).

[21] Paul Gallagher. 2020. URL: `https://github.com/tardate/LittleArduinoProjects/tree/master/Electronics101/INA226/HighSideMonitorBasics/WithRawWire`. (accessed: 08.09.2022) (cit. on p. 50).

[22] Adafruit. *Adafruit SSD1306*. URL: `https://www.arduino.cc/reference/en/libraries/adafruit-ssd1306/`. (accessed: 08.09.2022) (cit. on p. 65).

[23] Georg Icking-Konert Kai Liebich. *Task scheduler*. URL: `https://www.arduino.cc/reference/en/libraries/task-scheduler/`. (accessed: 08.09.2022) (cit. on p. 76).